The effect of matrix properties on the properties of Sheet Moulding Compounds

A study on material shrinkage behaviour and mechanical properties

Literature Study

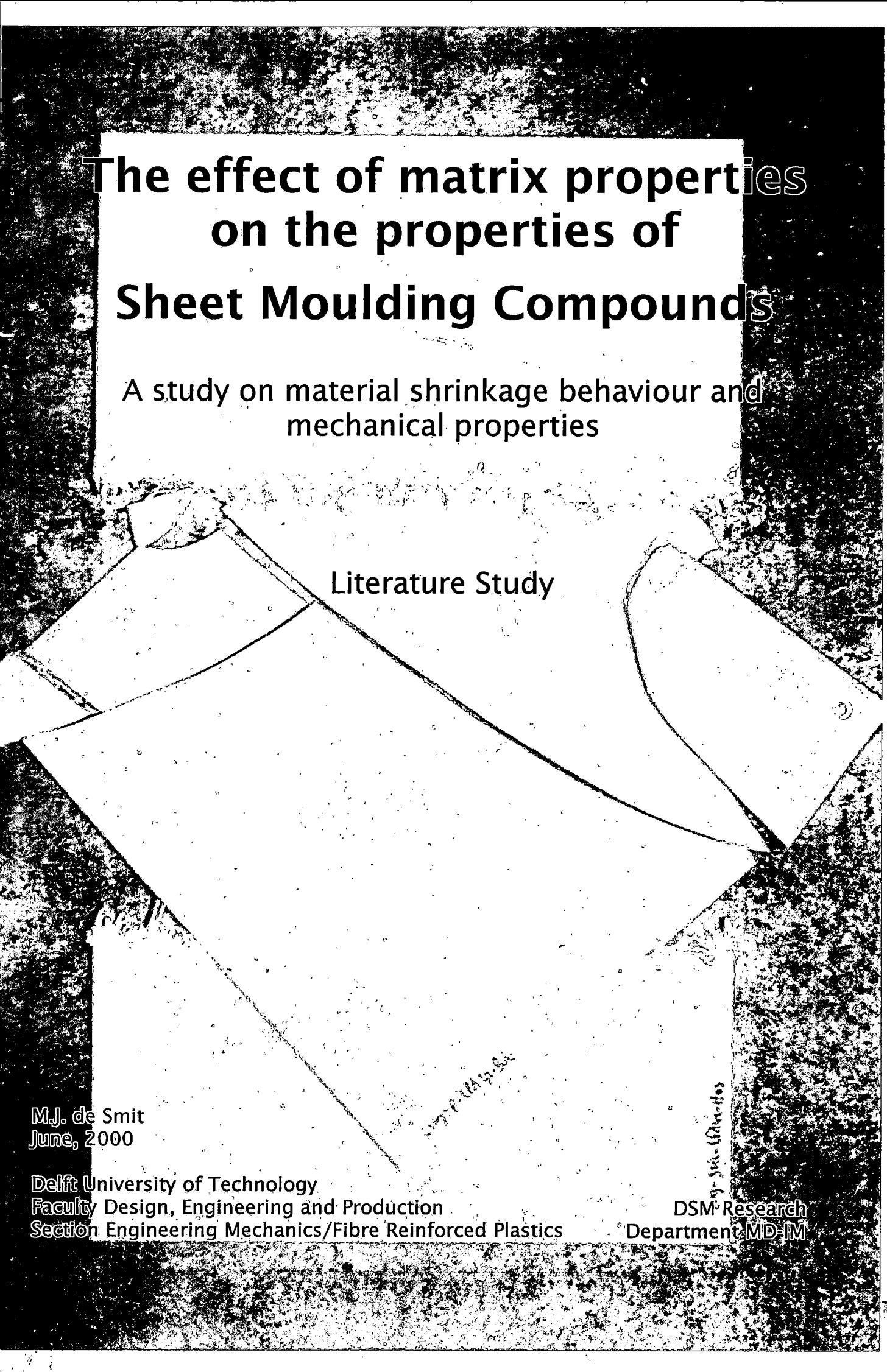

M.J. de Smit
June, 2000

Delft University of Technology
Faculty Design, Engineering and Production
Section Engineering Mechanics/Fibre Reinforced Plastics

DSM Research
Department MD-IM

Contents

Summary

A method is developed to evaluate Sheet Moulding Compound shrinkage properties and mechanical properties from mouldings of material without glass fibre reinforcement. This literature study describes issues that were important for this development.

Sheet Moulding Compounds (SMC) are sheets of paste compounded with randomly oriented discontinuous fibres. The paste primarily consists of thermosetting resin and filler. Additives are used to improve processability and performance of the material. SMC's are used in compression moulding processes where they cure in a hot mould of approximately 150°C under mould pressures between 40 and 100 bar.

From experimental results is concluded that the quality of the paste mixing process is important for moulding consistent and homogeneous paste plates on laboratory scale. This mixing process can be divided in three phases: mixing of liquid constituents, dispersion of solid powders and finally the addition of the thickener additive.

Mixing of low viscous miscible liquids requires high bulk flow to ensure good contacting. A propeller mixer is suitable for this purpose. High shear is only required if the formulation contains immiscible liquids. With the addition of the solid powders the apparent viscosity rises substantially and the rheologic behaviour changes from Newtonian to pseudoplastic.

Dispersion of solid powders requires high shear for good dispersion. Also high bulk flow is required to so that all material passes the high shear zone frequently. It might be necessary to use distinct devices for flow and shear induction.

Mixing of the miscible thickener paste into the high viscous pseudoplastic paste requires high bulk flow. High efficiency is important to prevent unnecessary temperature rise. A propeller with wide blades and large diameter can be used for this purpose.

The thickener additive changes the low viscous paste into a leatherlike material. The thickened paste behaves like a viscoelastic liquid. This thickened paste exhibits pseudoplastic behaviour. There is also a high dependence of the viscosity on temperature. At low temperatures the material is highly non-Newtonian at all shear rates. At higher temperatures the Newtonian region extends to higher shear rates.

The difference between paste and SMC is the incorporated glass. The reinforcement has a strong effect on the material response. Adding glass fibres increases the extensional viscosity two decades or more, but the shear viscosity remains of the same order of magnitude.

During the mould closure the SMC flows in uniform extension through the thickness of each layer with slip at the mould surface. This is a consequence of the lubricating layer along the mould walls and the high modulus of the SMC. Because a thermal gradient exists in the cross section of the SMC charge, the warmer external layers tend to flow faster than colder interior layers.

Paste exhibits low resistance to extensional deformation due to the absence of the glass fibre reinforcement. When paste is moulded, probably a thin low viscous lubricating layer is created. The low resistance against extension, the low driving force for inhomogeneous flow and the relative homogeneous temperature distribution through thickness will lead to a homogeneous lubricated extensional flow of the paste during the closure of the mould.

During the curing reaction a substantial change of the material characteristics is observed. The material transforms from a viscoelastic liquid to a viscoelastic solid. Volumetric changes occur due to thermal expansion and polymerisation shrinkage. At the end of the moulding cycle the moulding force is relieved. This decompression probably leads to an instant elastic relaxation and a time dependent viscous relaxation of the deformation.

Relations are derived for the calculation of SMC shrinkage properties and mechanical properties from measured paste properties. Mechanical properties of SMC can be calculated from the fibre and paste properties by imagining the composite as a laminate of infinitely many plies of infinitely small thickness with fibres oriented in all directions. First the mechanical properties of the unidirectional short fibre plies can be calculated with the formulas of Halphin and Tsai. Then the properties of the SMC can be calculated with the laminate theory as follows.

The expansion in longitudinal and transversal direction of unidirectional plies with unidirectional short fibres can be calculated from the expansion of the matrix and fibres with formulas of Shapery and Halphin. The expansion of the SMC can be calculated from the longitudinal and transversal expansion of the unidirectional ply by again assuming a laminate, consisting of many random oriented thin plies with unidirectional short fibres.

Introduction

A method is developed to evaluate Sheet Moulding Compound shrinkage properties and mechanical properties from mouldings of material without glass fibre reinforcement. This literature study describes issues that are important for this development.

Sheet Moulding Compounds (SMC) are sheets of paste compounded with randomly oriented discontinuous fibres. The paste primarily consists of thermosetting resin and filler. Additives are used to improve processability and performance of the SMC. SMC's are used in compression moulding processes where they cure in a hot mould of approximately 150°C under mould pressures between 40 and 100 bar.

An important issue in SMC-product development is the optimisation of SMC-properties for specific applications by changing the recipe of additives. In conventional SMC-research, for a small change in the formulation a considerable amount of SMC has to be produced because there are no machines for production of small batches. Then after moulding, change in properties can be measured. This way of optimising a formulation is very time and material consuming. Also changes of properties are masked by the fibre reinforcement.

In modern product development it is necessary to react fast and efficient on new market developments. A test method for evaluation of SMC-properties from paste plates without glass fibres makes it possible to optimise an SMC-formulation faster and more efficient. Important advantages of paste evaluation are saving of time and material and the ability of testing large series.

The literature study consists of four parts. The first chapter gives a description of SMC. Also a description is given of the functions and mechanisms of its constituents. The aim of the second chapter is to describe theoretical requirements a mixing method for SMC paste must meet to obtain good homogeneity, good dispersion of the solid components, and high mixing efficiency to prevent excessive temperatures. The reason for this research was that many inhomogeneities were found in moulded paste plates. The third chapter describes changes in rheological behaviour and volume during moulding of paste and SMC. Special attention is given to differences between paste and SMC behaviour. Good understanding of the moulding process is important because it will serve as basis for the modelling of shrinkage relations between pastes and SMC. Finally the fourth chapter describes the theory of mechanics of composites. Relations are derived for the calculation of SMC shrinkage properties and mechanical properties from measured paste properties. This theory is used in the final report.

This report does not answer a main question but has a descriptive function. For this reason the report does not end with conclusions. An exception is the second chapter. The main question of this chapter is which requirements a mixing method for SMC paste must meet to obtain good homogeneity. The conclusion is added at the end of the chapter.

1. Description of SMC

1.1 Description of SMC

Sheet Moulding Compound (SMC) is a type of composite material consisting of paste compounded with randomly oriented discontinuous fibres. The paste primarily consists of thermosetting resin and filler. Additional ingredients are used to enhance the performance and processing of the SMC.

For production of SMC, first all the ingredients, except the glass, are mixed together to form the paste. Then the paste is compounded with the glass fibres as illustrated in figure 1.1. The paste is transferred into two doctor boxes where it is deposited onto moving carrier films passing directly beneath. Glass fibre rovings are fed into a rotary cutter above the upper resin-covered carrier film where they are cut to length and are dropped onto the resin paste. Downstream from the chopping operation, the upper carrier film coated with paste is laid on top of the chopped fibres. The created sandwich layer with the chopped glass fibres in the middle is then sent through a series of compaction rollers where the glass fibres are wetted with the paste and excess air is squeezed out of the sheet. At the end of the SMC manufacturing process, the SMC is taken up on a storage roll or bi-folded.

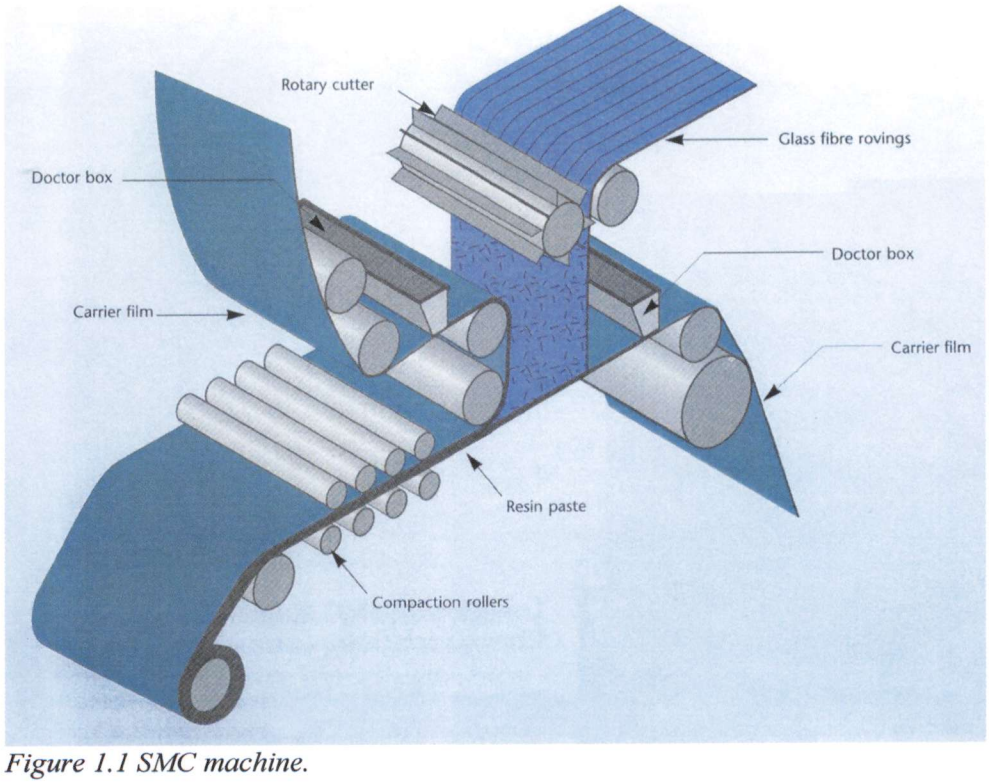

Figure 1.1 SMC machine.

The compounded sheets are then stored to age (maturation). This maturation period is necessary for the relatively low-viscosity paste to thicken chemically. The paste viscosity at the time of compounding is in the range of 40 to 100 Pa·s. The desired moulding viscosity is in the range of $50 \cdot 10^3$ to $150 \cdot 10^3$ Pa·s. This thickening makes the SMC easier to handle and prevents the paste from being squeezed out of the fibre blanket.

SMC's are handled in compression moulding processes. When the SMC is ready for moulding, the material is cut into pieces of predetermined size and shape. The cut pieces are then stacked and assembled into a charge pattern. This charge is then placed on the heated mould surface, which is usually heated to ca. 150°C. After the charge placement in the mould, the mould is closed and the SMC-charge is compressed. During the moulding cycle, which is about one to three minutes long, the pressure is maintained at about 50 to 100 bar.

Under the heat and pressure the SMC is turned into a lower-viscous liquid. The SMC flows to fill the mould cavity while the clearance at the mould shear edges allows the escape of air ahead of the flow front. When the mould is filled, glass fibres shut off the shear edges preventing low viscous material to pass through. The heat of the mould activates the polymerisation of the thermosetting resin, resulting in the solidification of the material.

1.2 SMC Components

In SMC-formulations, many variations in ingredients are possible. The principal thermosetting resins used in SMC are unsaturated polyesters and vinyl esters. Also epoxy resins and phenolics can be used. A new development is SMC based on melamine formaldehyde. There is also a great variety of additives, which are used to improve material properties and material characteristics.

The list of additives includes low profile additives (LPA), solvents for reducing viscosity and improvement of flow, wetting agents, initiators, accelerators, inhibitors, mould releasing agents, pigments and thickening agents. Furthermore various types of fillers can be used. The most commonly used fillers are calcium carbonate, alumina trihydrate, and hollow glass microspheres. Possible reinforcements of SMC are glass, carbon and aramid fibres.

In this paragraph the function and mechanism of the thermosetting resin and various other contents is described. Because the most common SMC is made, using chopped glass fibres for reinforcement, calcium carbonate as filler, and a thermosetting polyester combined with styrene as thermosetting resin. This description concentrates on additives used in these compounds.

Basic components of unsaturated polyester based SMC are listed below. There are more additives like fire retardants and UV-absorbers, but description of these is beyond the scope of this report. An indication of the composition of the UP-based paste is depicted in figure 1.2. The percentages are mass percentages.

- Unsaturated polyester
- Thermoplastic LPA
- Styrene
- Initiator
- Inhibitor
- Accelerator
- Releasing agent
- Filler
- Pigment
- Thickener
- Fibres

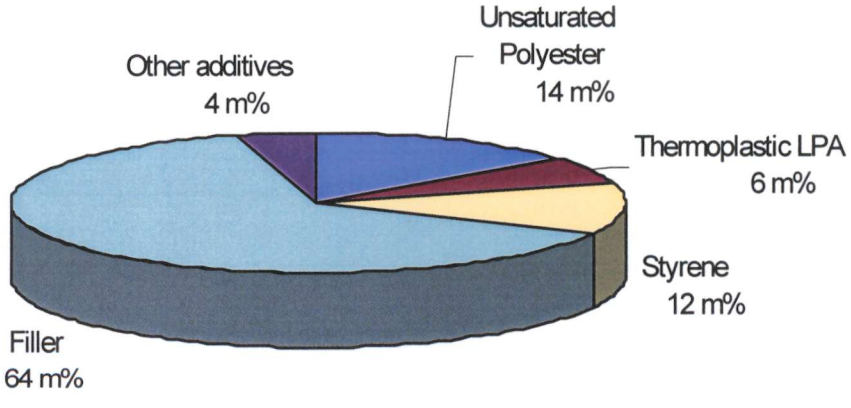

Figure 1.2 Composition of the UP-based paste.

Below a short description is given of the function and the mechanism of these components. Some components are described more in detail because their function or mechanism is important in the scope of the research after relations between paste and SMC.

Unsaturated Polyester

Unsaturated polyester is prepared by polycondensation of an unsaturated di-carbon acid with a di-alcohol. The reaction is schematically shown in figure 1.3.

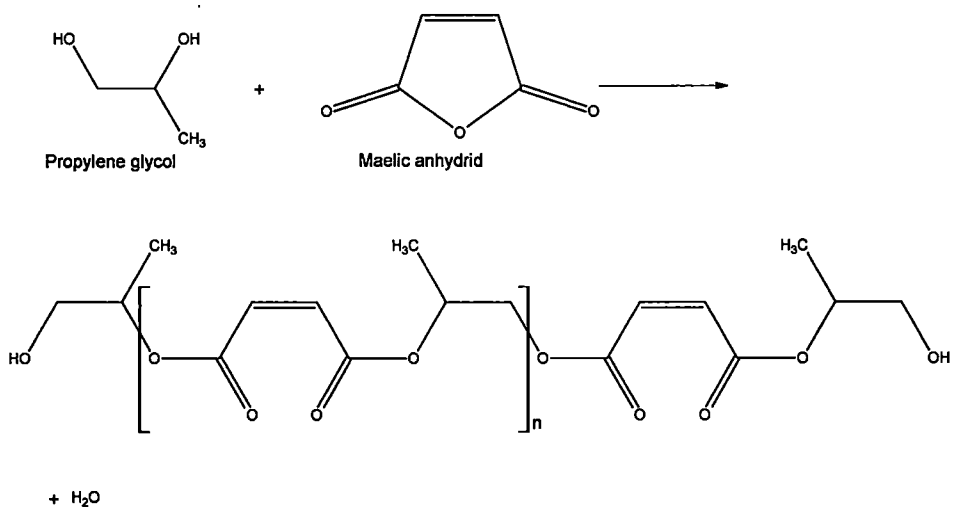

Figure 1.3 Preparation of unsaturated polyester.

Most used are polyesters of maelic anhydrid and propylene glycol. Saturated acids are added to modify the number of double bonds. The polymeric liquid is dissolved in a reactive monomer. Normally styrene is used. The styrene functions as solvent to lower the viscosity. The styrene also functions as cross-linking agent by linking polyester molecules at their double bonds. The unsaturated polyester cures by radical polymerisation as shown in figure 1.4.

Advantages of unsaturated resins are low costs and short curing times. Moderate composite properties and poor chemical and hydrolytic resistance are disadvantages of the UP resin.

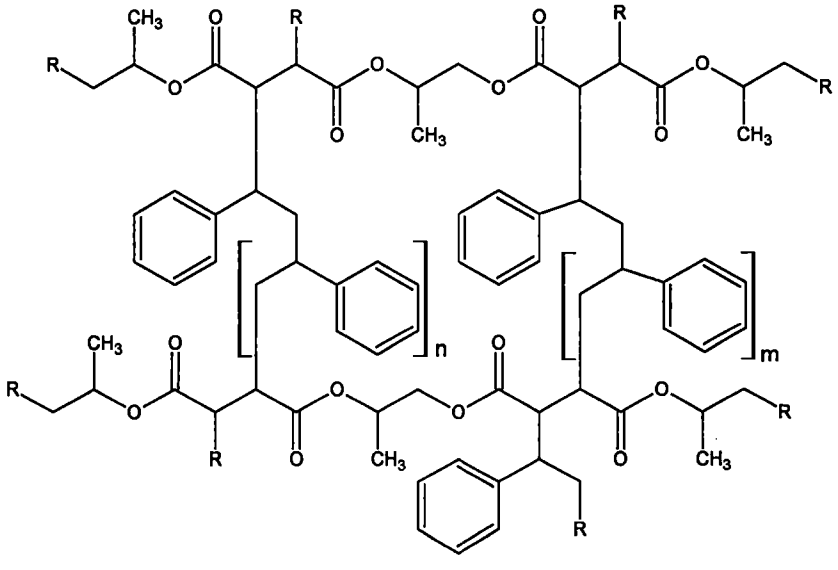

Figure 1.4 Curing reaction of unsaturated polyester.

Initiator
The unsaturated polyester cures by a free radical mechanism in which the double bond of the polyester chain reacts with the styrene. Organic peroxides are used to initiate this copolymerisation reaction by providing free radicals. At high temperature the peroxide dissects in radicals. These radicals break open the double bonds of the styrene and the unsaturated polyester.

Generally, the effectiveness of the initiator depends on its thermal decomposition rate at a given temperature and on the ability of the formed radicals to carry out the polymerisation reaction [ref. 4.].

Inhibitor
To prevent spontaneous polymerisation, an inhibitor is added to the paste. In general, inhibitors function by reacting with growing polymer chain radicals. A radical of low reactivity is produced that shows a reduced tendency for propagation [ref. 4.]. The most frequently used inhibitor is para-benzoquinone. Inhibitors are added to lengthen the storage life of the SMC, and also to modify the cure rate and magnitude of exotherms to prevent microcracking of thick moulding sections [ref. 4.].

Accelerators
To accelerate the production of radicals, accelerators are added. Accelerators catalyse the decomposition of the peroxides. Some accelerators are consumed so they are no catalysts. Accelerators are added to reduce the curing time during moulding. Often used accelerators are metal soaps like cobalt octoate.

Low Profile Additives
During curing of the unsaturated polyester, the volume of the material decreases. This decrease in volume during curing is referred to as polymerisation shrinkage. Shrinkage causes several problems like: [ref. 4.]

- poor surface appearance
- warpage of moulded parts
- internal cracks and voids
- sink marks on the surface opposite reinforcing ribs and bosses

Adding a thermoplastic or elastomeric phase can reduce the shrinkage. These additions are generally referred to as low profile additives (LPA). The LPA reduces shrinkage which results in better surface quality (less sink marks and waviness), less warpage and cracking. Using LPA can also have negative side effects like unequal spreading of pigments in LPA and UP (marble effects) and migration of the LPA-phase out of the compound (sheet tackiness, surface cracking).

Different LPA additives are can be used and also mixtures of LPA additives are possible. Various thermoplastics and elastomers have been found to give varying levels of shrinkage control. For these different additives, several different mechanisms for shrinkage control have been offered. The mechanistic suggestions that are reviewed in this section are obtained from microscopic examination [ref. 2].

Certain LPA-additives form a two-phase system. As the temperature rises during cure, the LPA-rich phase expands thermally and counteracts polymerisation shrinkage. After polymerisation spherical dispersed voids appear because the LPA rich phase shrinks due to homopolymerisation and thermal shrinkage.

Other LPA-additives form a Single-phase system. Crosslinking during curing induces phase separation that leads to creation of additional internal volume. After polymerisation and

during cooling, shrinkage is minimised relieving shrinkage stresses internally by microcracking or deformation of the weak LPA phase. High dispersity of the thermoplastic phase or large interfacial area seems to increase the ability of reducing shrinkage. Microcracking can be postponed ore even be prevented.

Two-phase systems are better pigmetable because continuous microcracks which appear in single phase systems make the surface appear more white. Spherical cracks that appear in two-phase systems are hardly visible so the material has better appearance.

Examples of LPA-additives:

Polystyrene (PS)

A two-phase system is formed of PS-rich droplets in the matrix of UP. After copolymerisation of UP residual styrene in PS rich phase starts to homopolymerisate. PS agglomerates start to shrink. Internal stresses are relieved by formation of spherical cracks (voids) with PS balls inside.

Styrene/Butadiene (SBS) triblockcopolymer (rubber)

A two-phase system is obtained consisting of a fine dispersion of SBS rich droplets. After copolymerisation microcracking occurs due to copolymerisation of styrene in droplets. Almost the same as PS but dispersed more homogeneously

Polymethylmethacrylate (PMMA)

A two-phase system is obtained consisting of spherical droplets of PMMA rich phase. During copolymerisation, also phase separation occurs in the PMMA-rich domains. Microcracking occurs in the PMMA domain due to copolymerisation.

Polyvinylacetate (PVAc

Normally a single-phase system is obtained. Crosslinking induces phase separation. A dispersion of UP surrounded by a PVAc-rich phase is obtained. Shrinkage stresses due to polymerisation are relieved by microcracking in the weak PVAc-rich phase.

Saturated Polyester (SP)

A single-phase system is obtained. Crosslinking induces phase separation. During cooling shrinkage stresses can cause deformation or microcracking in SP-rich phase.

Filler

Figure 1.2 shows that the filler component is a main ingredient of the paste [ref1.]. Fillers affect the material properties in many ways. Usually fillers are used to modify physical properties and to reduce costs. Fillers increase the paste viscosity and modify the rheologic behaviour. Furthermore the filler reduces shrinkage, and increases the stiffness and hardness of the moulded material. The filler also forms a barrier to phase separation.
Important factors for selection of fillers are volume cost, specific gravity, particle size distribution, packing density and oil absorption. The ideal filler has a low specific gravity and a definable chemical composition. It is non-abrasive, pure, white and non-porous. Low oil absorption is important because viscosity rises with increasing oil absorption. A combination of high loading with low viscosity is desired to obtain good wetting of fibres and good flow properties. Low cost is of course an important demand. Densities of various filler materials are listed in table 1.1.

Filler	Specific gravity [g/cm^3]
$CaCO_3$	2.71-2.93
Kaolin clay	2.60
Talc	2.70
solid glass spheres	2.50
hollow glass spheres	0.40
Alumina trihydrate	2.42

Table 1.1 Density of common filled materials.

Available types of fillers are calcium carbonate ($CaCO_3$), kaolin clay and talc. The most used are calcium carbonates. Hollow glass spheres and alumina trihydrate ($Al_2O_3 \cdot 3H_2O$) are examples of functional fillers. Hollow glass spheres are used for weight reduction. Alumina trihydrate works as flame retardant since the water of hydration in its molecule is released at elevated temperatures (ca. 220 C°).

Releasing agent
Function of the releasing agent is to prevent adhesion between the SMC and the mould surface (mould sticking). Polyester resins are polar and therefore they have an affinity for metal surfaces. Most release agents are long-chain fatty acids and their salts. On heating they melt and migrate to the surface as a secondary phase. Usually a release agent is chosen with a melting point just below the curing temperature. This prevents marring on the surface due to premature melting. Most used releasing agents are zinc stearate and calcium stearate [ref. 1.].

Pigment
In the experimental part of this research, pigments are used for visualisation of flow patterns moulding multicoloured charges. This application is described in chapter 3. Because in these applications, the effects of the pigment on the material properties must be known, a short description is given below [ref.5.].

Pigments are divided in three basic families: dyes, organic pigments and inorganic pigments. Dyes dissolve whereas other colorants are small coloured parts. Dyes have a low specific gravity and a high tinctorial strength. Due to their poor heat resistance and their tendency to migrate, they are seldom used in polyester compounds. Organic pigments have good brightness and brilliance. Their colours generally are not so bright as those obtained from dyes. Other properties are limited solubility, low specific gravity and high oil absorption.

Inorganic pigments usually are natural or syntetic metallic oxides, sulfides, and other salts. They are superior to organic pigments and dyes in heat resistance, light stability, weather resistance and migration resistance. Normally they produce opaque colours. Other properties are high specific gravity, low oil absorption and good chemical resistance.

A pigment requires good light-fastness, good dispersibility and neutrality to polymerisation. Some pigments have a strong effect either in accelerating or inhibiting the curing of polyesters. Of several pigments the effect on the curing reaction is listed in table 1.2.

Pigment	Colour	Form	Effect on curing reaction
Cadmium Salts	Greenish yellow to orange	Concentrate	Accelerators
Carbon Black	Black	Powder	Inhibitor
Iron Oxide	Red	Powder	Accelerator
Copper Salts			Inhibitor/Accelerator (depending on concentration)
Aluminium Salts			Accelerators
Titanium Dioxide	White	Powder	Slight Accelerator
Phthalocyanine Green	Green	Concentrate	Slight Inhibitor
Organic Dyes and Pigments		Concentrate	Inhibitors
Kaolin Clays		Concentrate	Slight accelerators

Table 1.2 Effect of curing reaction on different types of pigments.

Thickener

[ref. 3] [ref. 4.] A very important additive is the thickener. The thickener changes the low viscous paste into a leatherlike material. The viscosity increase makes the SMC easier to handle and prevents paste from being squeezed out of the fibre blanket. Initially a low viscosity is needed for good wetting of the fibres. After maturation a high viscosity is needed for tacky free and easy to handle sheets.

It is very important that the thickening process is predictable and reproducible with maximum consistency. For this it is necessary to understand the basic chemistry involved, as well as sources of variations. For this reason a short description of the mechanism of the thickening process is given in this section.

Thickening is a time dependent process. A typical thickening course in time for a paste is depicted in figure 1.5 [ref.3]. In this figure three regions can be distinguished. Thickening is inhibited in the first period directly after the addition of the thickener. This inhibition time is important for good wet-out of glass fibres in SMC. In the second region a rapid increase of viscosity takes place. This period must be as short as possible for low stock levels. Finally in the third period, the viscosity reaches a plateau where the viscosity only increases slowly. A constant viscosity is desired over long time for a large moulding window. This is the time in which parts can be moulded within their specifications.

Common thickeners used in SMC formulations are oxides and hydroxides of magnesium or calcium [ref.3][ref.4.]. Mostly used thickening agent is magnesium oxide (MgO). Use of MgO is assumed in the explanation of the thickening mechanism below.

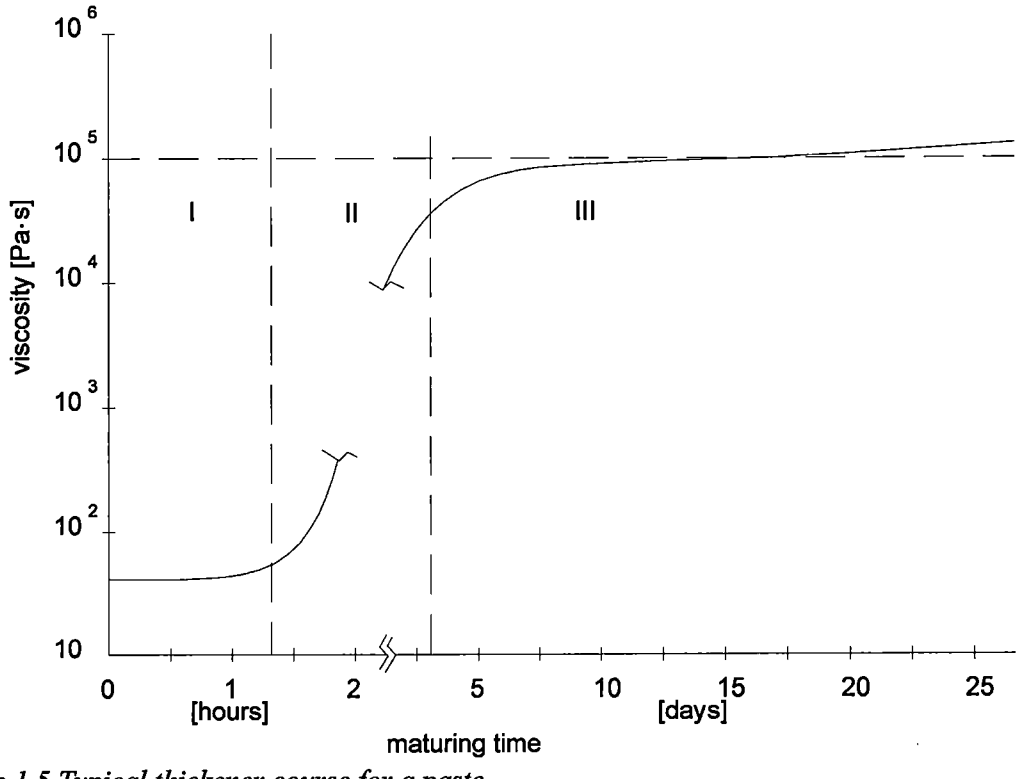

Figure 1.5 Typical thickener course for a paste.

The thickening reaction takes place in two stages. A basic salt formation reaction between carboxilic end-groups of unsaturated polyester and insoluble MgO occurs in the first stage. The basic salt can be transformed into a neutral salt by reaction with the second carboxilic end-group of another polyester molecule. This linear chain extension results in a higher paste viscosity.

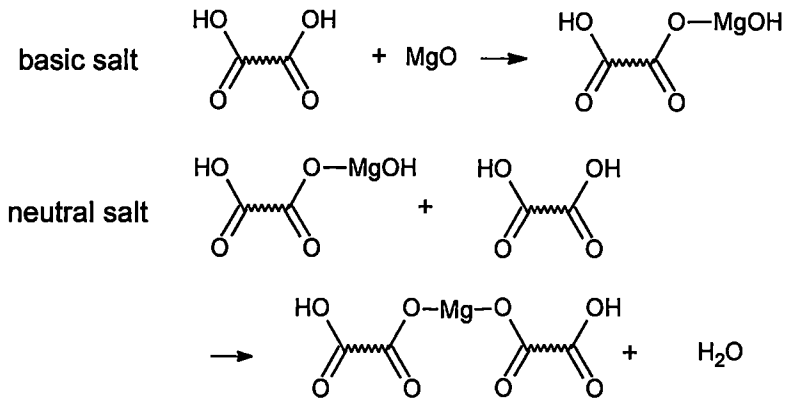

Figure 1.6 Reaction schemes of salt formation.

The second stage involves the creation of bridging networks that further increase the paste viscosity. Two different mechanisms of network formation can be distinguished. The first type involves formation of hydrogen bonds between carboxyl and ether oxygens figure 1.6. Because each polymer molecule has many of these hydrogen bonds, a large network can be formed. The second reaction is the formation of complexes between the ester groups in the polyester chains and/or hydroxyl end-groups and the magnesium atom figure 1.7. A complex consists of a central atom or ion with one ore more molecules or ions bound to it with a free electron couple.

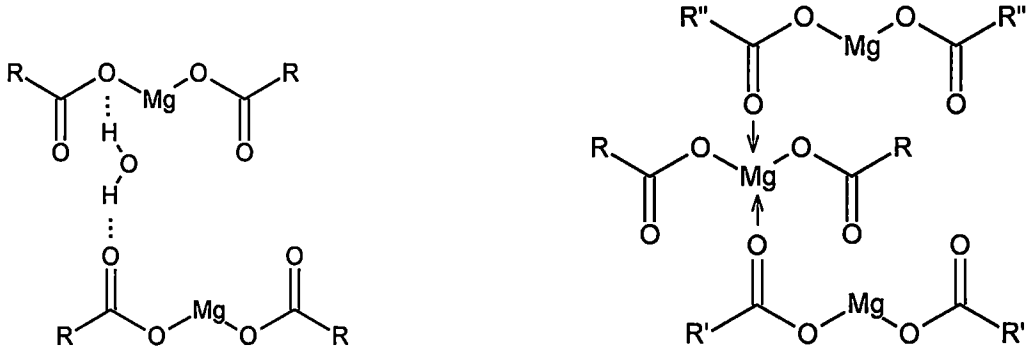

formation of hydrogen bonds

formation of complexes

Figure 1.7 Formation of complexes.

Many variables influence the thickening rate of SMC formulations. Moisture for example is known to accelerate the thickening process and lower the final plateau viscosity. Also the raw materials used in SMC can be a major source of variation. In the experimental part of this research, variations were made in the formulations of the tested materials. Influences of several contents are described below.

First of all the thickening rate is influenced by the thickener type, purity and amount. Also the molecular weight and acid content of the unsaturated polyester resin influences the thickening rate. Even different lots of the same resin have been found to exhibit different thickening rates [ref. 4.]

Saturated polyester LPA contains carboxilic end-groups, so it participates in the thickening reaction. Carboxyl groups are also introduced to other LPA additives to prevent physical separation. This allows participation of the LPA in the thickening reaction and avoids phase separation [ref. 4.]. This can have a profound effect on the thickening rate and the final

viscosity level because the molecular weight of most LPA polymers is considerably above that of unsaturated polyester.

It has been observed that the chemical thickening can have a marked negative effect on the LPA performance [ref. 4.]. As explained earlier in this section, the formation of two phases is critical for the activity of the LPA. The chemical thickening possibly effects this phase formation.

The type of filler material can also have a large effect on the thickening reaction. It is even possible to introduce differences by simply changing from one calcium carbonate to one other [ref. 4.]. Metal stearates, used as releasing agents, are also active in the thickening reaction. They are not pure compounds but complex mixtures of metal oxides and carboxyl acid, and they seem to act as thickener themselves [ref.1.].

For thickening, usually a paste is used of magnesium oxide dispersed in a non-reactive unsaturated polyester resin without carboxylic end-groups to prevent premature thickening. Use of predispersed thickeners has many advantages. They are for example not dusty, more easily and homogeneously incorporated into the SMC, and less susceptible to moisture absorption [ref. 4.].

Glass fibres

This report describes issues that are relevant for the research after shrinkage relations between paste and SMC. The main difference between paste and SMC is the presence of the fibre reinforcement. For this reason several issues concerning the glass fibre reinforcement are described below.

Glass fibre reinforcement is essential for use in SMC to achieve the desired mechanical properties and dimensional stability. Usually E- (electrical) glass is used in SMC. A typical E-glass composition is listed in table 1.3. Typical physical properties of the E-glass fibres are listed in table 1.4.

E-glass composition [%]	
Silica (SiO_2)	52-56
Calcium oxide (CaO)	16-25
Alumina oxide (Al_2O_3)	12-16
Boron oxide (B_2O_3)	5-10
Magnesia oxide (MgO)	0-5
Alkali Oxides (Na_2O and K_2O)	0-2
Titanium dioxide (TiO_2)	0-0.8
Ferric oxide (Fe_2O_3)	0.05-0.4
Fluorine (F_2)	0-0.1

Table 1.3 Typical E-glas composition

Physical properties of E-glass	
thermal expansion coefficient	$1.6 \cdot 10^{-6}$ °C^{-1}
Tensile strength at 50% relative humidity at 22.2°C	1.4-3.4 GPa
Elastic modulus E	72.4 GPa
Bulk modulus K	34.5 GPa
Poissons ratio ν	0.22
Elongation standard at break	3-5%
Elastic recovery	100%
Average stiffness	28.4 N/tex
Specific gravity	2627 kg/m^3

Table 1.4 Physical properties of E-glass

Glass fibre filaments can be characterised by their diameter. In SMC applications the most widely used average filament diameter is 13.5μm. The filaments are gathered into various numbers of strands and wound onto a bobbin. The strand can be characterised by its size, number of filaments and by the shape of its cross section.

Finally a number of strands is wound together into a continuous roving. For application in SMC these rovings are fed to the fibre chopper in the SMC machine as explained in paragraph 1.1. Usual chop lengths are 25 mm. Glass fibre rovings are characterised in many ways. Important attributes are yield, strand dispersion, strand geometry, and type of sizing. The roving yield is a measure of weight per unit length. The ISO designation tex is used for this linear density. Tex is defined as the mass in grams of one km of roving. The strand size is usually measured indirectly by measuring the roving yield and the number of strands in the roving (end count).

A sizing is applied to the glass fibre filaments directly after production. Then the sizing is cured and water is removed from the glass fibres in an oven. A sizing is a complex mixture of coupling agents, film formers and lubricants. Sizings have many functions of which the most important are the following:

1. Adhering the fibres together to protect the brittle glass from abrasion.
2. To lubricate the fibres in subsequent processing.
3. To impart anti static properties to the glass fibre.
4. To provide a good chemical bond between the glass fibre and the polymer matrix.

The type of sizing plays a major role in SMC performance. An important indicator is its solubility in the styrenated resin. The wetting potential and the degree of filamentation of the glass strands are largely controlled by the styrene solubility of the sizing. For optimum mechanical properties of the SMC, complete encapsulation of the glass fibres by the matrix material is desired. So optimum stress transfer is achieved by high styrene solubility. On the other hand, integral rigid strands have the best ability to flow with the resin. The ability to flow with the resin is critical for an even glass distribution. Soft and filamentised strands tend to yield and agglomerate during flow [ref. 4.]. To ensure a uniform glass distribution, minimum warpage, and optimum surface quality, the integrity of the strand must be maintained. For this reason, low styrene solubility is desired for automotive applications.

Literature

1. Burns, R., *Polyester Molding Compounds*, Marcel Dekker Inc., New York ,1982.
2. Goudswaard, I., A light microscopy study of shrinkage control in UP resin, DSM Research N 95.1589, Geleen 1995
3. Goudswaard, I., *SMC moulding window*, DSM Research NC 93.2922, Geleen 1993
4. Kia, H. G., *Sheet Molding Compounds, Science and Technology*, Hanser Publishers, USA, 1993
5. Mallick, P.K., *Fiber reinforced composites, materials manufacturing and design*, Marcel Dekker Inc., New York, 1988.
6. Mallick, P.K., Newman S., et al., *Composite Materials Technology, Processes and Properties,* Carl Hanser Verlag, Munich, Vienna, New York, 1990.
7. Meyer, Raymond W., *Handbook of Polyester Molding Compounds and Molding Technology,* Chapman and Hall, New York, 1987.
8. Reinhart T. J. (Eds.), *Engineered Materials Handbook, Volume 1 Composites*, ASM International USA, 1987
9. Young R.J. , *Introduction to Polymers*, Chapman and Hall, Great Brittain,1987

2. Preparation of paste

2.1 Introduction

The aim of this chapter is to describe theoretical requirements a mixing method for SMC paste must meet to obtain good homogeneity, good dispersion of the solid components, and high mixing efficiency to prevent excessive temperatures.

In experiments of paste plate mouldings it was found that paste plates contain inhomogeneities. These inhomogeneities cause thickness variations in the plate surface. Because from measurements on these paste plates, SMC material characteristics must be predicted, it is important that the method yields consistent and homogeneous products. Also for applications of SMC in the automotive industry homogeneity can be very important because the inhomogeneities can have bad influence on the surface quality. It is possible insufficient mixing causes these inhomogeneities.

The preparation of SMC paste starts with the mixing of low viscous resins and other liquid constituents. Solid filler material and the releasing agent are added when the liquids are well mixed. The addition of the large amounts of solid powers leads to a substantial viscosity increase and a change of rheologic behaviour. This change of properties makes the paste mixing a complex process.

In this section first several general aspects of mixing are discussed. Then this description of mixing is used to describe the requirements a mixing method for SMC paste must meet.

2.2 Mixing introduction

The term mixing is applied to processes used to reduce the degree of non-uniformity, or gradient of property in a system such as concentration, viscosity, temperature and so on. The main principle that lies at the bottom of the mixing mechanism is to increase the interfacial area between the media that must be mixed [ref.2]. The mixing process can be divided in convection and shear. If media are miscible the final phase is diffusion.

Mixing is a complex process which makes the practice of designing mixers a difficult task. For non-Newtonian flows the design problem contains a two-fold complexity: complicated geometries such as the tank and impeller systems as well as complicated fluid rheology such as elasticity and a deformation-rate dependent viscosity.

Depending on fluid properties and mixing conditions the flow in mixing vessels can be laminar or turbulent. Laminar mixing is usually associated with high viscosity liquids (>10Pa·s) which may be either Newtonian or non-Newtonian. A laminar flow has a so-called layered structure. The mechanisms shear and elongation result in an increase in interfacial area. The ultimate homogeneity of miscible fluids can only be reached with molecular diffusion. In case of liquids of high viscosity this is a slow process. A necessary condition for effective mixing in laminar flow is crossing of streamlines.

For low viscosity liquids, the bulk flow pattern in mixing with rotating impellers is mostly turbulent. In a turbulent flow, the combination of mixing conditions and fluid properties lead to eddying. Eddy diffusion occurs throughout the vessel but at maximum in the vicinity of the impeller.

Fluid properties and flow conditions, which determine the flow type, can be quantified in the Reynolds number (Re). The Reynolds number quantifies the ratio between the kinetic energy and the friction forces in the flow.

$$\mathrm{Re} = \frac{\rho v D}{\eta} \qquad (2.2)$$

ρ	= Density	[kg/m^3]	
v	= Average speed	[m/s]	
D	= Length dimension	[m]	(In case of mixing, D is the impeller diameter)
η	= Dynamic viscosity	[Pa·s]	

For mixing the value of Re where the flow changes from laminar to turbulent can not be indicated precisely. The flow type is also very depends on the mixing device. Roughly the regions can be divided as follows:

Re<100	100<Re>10^4	Re>10^4
Laminar	Transition	Turbulent

2.3 Rheologic behaviour

The rheologic behaviour has great influence on the mixing behaviour. Newtonian and non-Newtonian behaviour can be distinguished. The viscosity of a Newtonian liquid is independent of shearing ratio. It will develop flow at the smallest shear stress.

Non-Newtonian fluids are rheologically complex fluids that exhibit one of the following features:

- Shear rate dependent viscosities in certain shear rate ranges with or without the presence of an elastic behaviour.
- Yield stress.
- Time dependent viscosities at fixed shear rates.

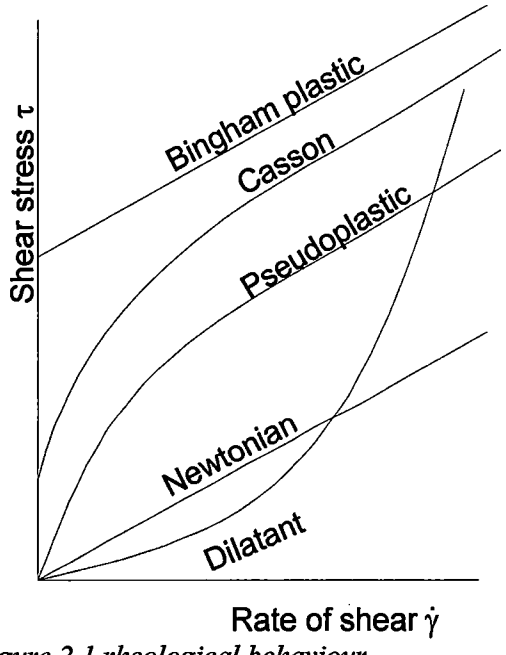

Figure 2.1 rheological behaviour

Examples of non-Newtonian liquids are:

- Plastic liquids or Bingham liquids: these fluids do not flow unless the stress applied exceeds a minimum yield stress
- Pseudoplastic liquids (shear-thinning): These fluids exhibit shear thinning behaviour. They depict a decrease in viscosity with increasing shear rate.
- Dilatant liquids (shear-thickening): these fluids exhibit shear thickening behaviour. The viscosity increases with increasing shear rate.
- Casson liquids: exhibit a combination of plastic and shear thinning behaviour.
- Viscoelastic fluids: show partial elasticity. They can show partial elastic recovery upon the removal of a deforming stress.

High viscosity fluids often exhibit non-Newtonian behaviour. Polymer liquids for example often exhibit pseudoplastic behaviour. Also systems of solids dispersed in liquids often show non-Newtonian behaviour, even if the liquid phase is Newtonian in behaviour. At very low solid concentration very little deviation from Newtonian behaviour will be observed. the slurry often starts to exhibit plastic or pseudoplastic behaviour with increasing level of solid particles.

2.4 Types of mixing

Many different types of mixing operations can be distinguished. Some examples are blending of miscible liquids, suspension of solids, dispersion of immiscible liquids or solids in liquids, heat transfer, dissolving solids in liquids, and gas dispersion. Many mixing applications involve a combination of more than one of these. The various different mixing operations desire different mixing conditions. In this section, the types of mixing which occur in the paste preparation, and their required mixing conditions will be discussed. The following types of mixing in the paste preparation can be distinguished:

- Mixing of miscible liquids
- Mixing of immiscible liquids
- Liquid-solid mixing

Mixing of *miscible* liquids is the simplest type of mixing. The mixing of two miscible phases requires high bulk fluid flow to ensure good contacting while generating very little shear that could emulsify the two components of the mix. Agitation requirements increase with increasing viscosity. Problems can pose when liquids have vastly different viscosities [ref.11] [ref. 5].

Mixing of *immiscible* liquids involves dispersion of one phase as tiny droplets in the second liquid which forms a continuous phase. Initially spherical drops are stretched by hydrodynamic forces acting on the drop. The hydrodynamic stresses must be large enough to overcome the surface tension that tends to return the drop to a spherical shape. This indicates that high shear or intensive agitation are required for effective dispersion of one phase into the other. Stretched drops eventually break due to surface tension driven instabilities. The driving force behind this process is provided by the interfacial tension minimising the surface area.

The ratio of deforming viscous forces to resisting interfacial forces is called the capillary number Ca. The viscosity ratio between the dispersed and the continuous phase is called p. The degree of deformation and whether or not a drop breaks is completely determined by Ca, p, the flow type and the initial drop shape and orientation [ref.5]. Bentley and Leal (1986) have shown that it is easiest to stretch drops when $p \approx 1$ and that elongational flow is more effective than simple shear flow. Experiments of Tjahjadi and Ottino, (1991) showed that the equilibrium size distributions corresponding to high viscosity drops are more non-uniform than those corresponding to low viscosity ratios, and that, in general, the mean drop size decreases as the viscosity ratio p increases. Low viscosity drops extend relatively little before they break resulting in the formation of large droplets. High viscosity ratio drops stretch substantially before they break in very small fragments.

During mixing dispersed drops can also collide and if the film between the drops break, this can lead to coalescence. The balance between break-up and coalescence determines the drop size distribution in the mixture. Coalescence is commonly divided in three sequential steps (Chesters, 1991). First collision or close approach of two droplets occurs. Then the liquid between the drops is squeezed forming a film. Finally the film drains. If a critical film thickness is reached, the film ruptures as a result of van der Waals forces, and the drops coalesce.

The mobility and rigidity of the interface determine the rate of drainage. The mobility of the interface is essentially determined by the viscosity ratio p. Coalescence is directly proportional to the continuous phase viscosity because a higher viscous interface is less mobile. The rigidity of the interface is determined by the interfacial tension and determines the degree of flattening of the drop. Drainage time is shortest when the drops are rigid. Drainage time decreases with drop size so smaller drops are more likely to coalesce than larger ones. Coalescence is also more likely to take place in regions of low shear rate.

Liquid-solid mixing involves dispersion of solids in liquids into a homogeneous two phase mass. This type of mixing is important in the formation of composite materials where fine particles or short fibres must be dispersed in liquids. Mixing together of particulate solids is a

very complex process. It is very dependent on the character of the particles, the size distribution of the particles and on the properties of the components.

Powders dispersed in liquids consist of agglomerates. Agglomerates are collections of aggregates, which in turn are composed, of primary particles. The agglomerates break down due to flow and aggregates do not. The process of dispersion of a powder into a liquid involves several stages. First the solid is incorporated and wetted by the liquid. This wetting may consist of adhesion of the medium to the solid, immersion of the solid into the fluid and spreading of the liquid in the porous solid. Furthermore fragmentation of agglomerates into aggregates and aggregation occur.

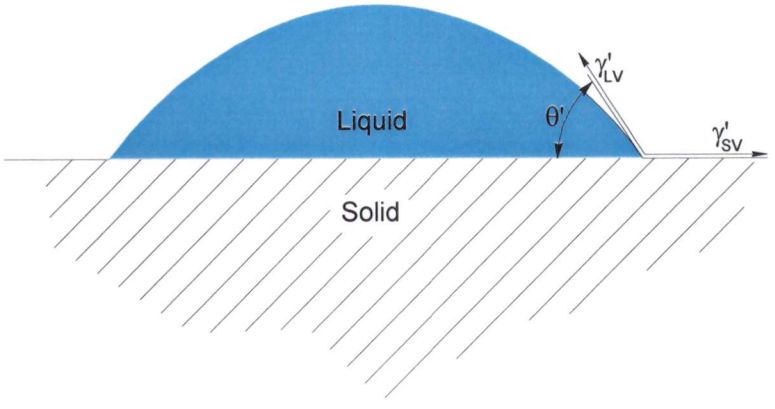

Figure 2.2 Contact angle.

Wettability affects the ease of dispersion of solid contaminants in the resin. The wetting of a solid by a liquid is dependent upon the relative interfacial energies among the solid, liquid and vapour phases as shown in figure 2.2. The contact angle θ' of the liquid drop on the flat surface is given as:

$$\cos\theta' = \frac{\gamma'_{SV} - \gamma'_{LS}}{\gamma'_{LV}} \qquad (2.2)$$

Where γ' is the interfacial energy and subscripts S, L and V refer to solid, liquid and vapour phases, respectively [ref.7]. Good wetting is obtained when the contact angle is zero. From this can be derived that good wetting occurs when:

$$\gamma'_{LV} + \gamma'_{LS} - \gamma'_{SV} < 0 \qquad (2.3)$$

It thus seems logical to aim for situations where the critical surface tension values of the solid surface are considerably less than those of the polymer. Wetting can be improved by suitable surface treatment of the solid with a coupling agent that improves the adhesion. In reality there are adsorbed gases on the on the solid surface leading to an increase in the contact angle. Also the solid surface is not smooth leading to a decrease in contact angle. [ref.7]

Fragmentation of agglomerates may be caused by several mechanisms, for example application of direct compressive loads, particle-particle and wall-particle impacts or by hydrodynamic forces. The agglomerate strength has great influence on the fragmentation. This agglomerate strength is not a material property but depends on internal structure, degree of compaction, moisture and many other variables. The agglomerate owes its cohesive strength to interparticle bonds due to electrostatic charges, van der Waals forces, or moisture [ref.5].
Fragmentation may be divided into two modes of break-up, rupture and erosion. Rupture refers to breakage of agglomerates into several elements of comparable size [ref.5]. Erosion

refers to gradual shearing off of small fragments from larger agglomerates. The most relevant mechanism depends on the mixer type. Erosion requires low energy input and occurs over long time scales. It dominates dispersion when stresses are low. Rupture occurs within a short time and requires high energy input. In case of high shear or intensive agitation, rupture dominates. In flows with spatially varying shear rates, erosion occurs in all regions of the flow while rupture only occurs during a visit to a high shear zone. Rupture is more likely in simple shear flow as compared to extensional flow since the agglomerate rotates in a simple shear flow and it experiences the entire range of stresses possible [ref.5].

2.5 Mixing regions

Three kinds of mixing system can be distinguished in a mixing system [ref.9]:

- Active mixing region
- Stagnant regions
- Isolated mixing regions (IMR)

In the *active mixing region* the material moves the fastest and material from every part of the region interpenetrates exponentially quickly. For good mixing, the active mixing regions must dominate. *Stagnant zones* are separated from the primary mixing zones by wall-attached separation streamlines. Material inside such regions moves slowly with respect to the primary flow. Contribution or even presence of stagnant zones can be minimised by altering the geometry of the system. Examples may be recirculating vortices behind the flow past a cylinder, multicellular flows in deep cavities or flows past contractions and steps. Examples are depicted in figure 2.3.

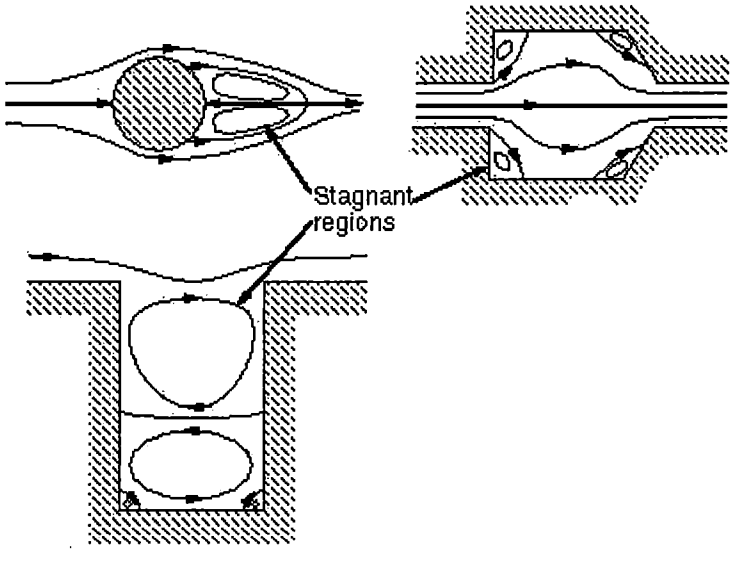

Figure 2.3 Examples of stagnant regions.

Isolated mixing regions (IMR's) are qualitatively different from stagnant regions in three respects:

- they are typically away from boundaries
- they are not identifiable by low flow speed
- they may exhibit mixing within themselves

Like stagnant zones the IMR's do not exchange material with the active mixing regions and therefore they can present a substantial obstacle to global mixing. Examples of IMR's are depicted in figure 2.4. Figure 2.4a shows an example of an IMR in a 3D situation of an impeller in a mixing vessel. Figure 2.4b shows an example of an IMR in a simple 2D situation of two eccentric rotating cylinders.

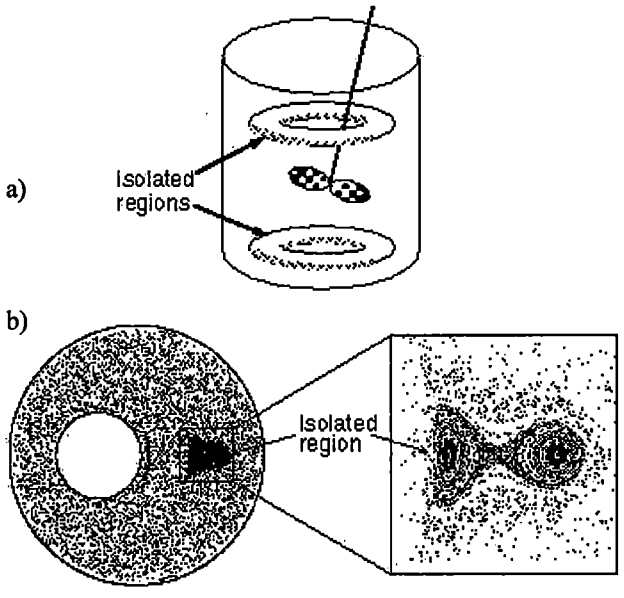

Figure 2.4 Examples of Isolated Mixing Regions.

An IMR can be formed or destroyed by slightly altering the flow. This can be done by means of changes in geometry. Driving a system faster does not imply better mixing. Islands survive and do not go away. For a non-Newtonian fluid, the viscosity is a function of the shear rate. Consequently for non-Newtonian flow, the speed of the boundaries plays an important role in the dynamics governing the mixing. In general, the overall effect of a shear thinning viscosity is a decrease in the amount of mixing in both the rate and extend. A shear thinning viscosity is found to result in formation of IMR's [ref.4].

2.6 Mixing devices

In this section, the features of common used mixer types are described. For the enormous variety of mixing duties, a wide range of mixing equipment is available. The wide variety in process demands has lead to the development of a great number of distinct mixer types. The lack of standardisation and design codes has made the variety in mixer types even more extensive.

2.6.1 Impeller in mixing vessel

[ref.10] The most commonly used method of mixing is the application of a mechanical driven impeller in a vessel. This type is also the most common used impeller for paste preparation. A mixing impeller is any device mounted on a rotating shaft that circulates materials in a vessel to achieve the desired result. The power applied by any mixing impeller produces a pumping effect and a velocity head. The fluid head defines the agitation intensity in the immediate discharge zone of the impeller, which is proportional to shear rate or turbulence.

Either the flow component or the shear component can be emphasised so that a large flow/small head or a large head/small flow can be produced with the same power input. Important parameters that determine the power input, flow patterns, and flow/shear ratio of a rotating mixing impeller are listed below:

- The rotor diameter and speed.
- Density and viscosity.
- Rheological behaviour [Newtonian or non-Newtonian].

- Geometry of the impeller.
- Design of the mixing vessel.
- Location of the impeller in the mixing vessel.

Impellers are available in many different geometries. They are categorised by their ability to dissipate energy in a combination of flow, shear and pressure. Each impeller has a primary function. Depending on the application of the impeller, components of the other functions must be implicated.

Flow impellers provide good contacting and top to bottom motion throughout the vessel. These impellers are used for flow controlled applications in which the flow generated has a direct result on the outcome of the process. For example a mixing two miscible phases which requires high bulk flow to ensure good contacting while generating very little shear that could emulsify the two components of the mix [ref.10]. Shear impellers produce a high level of energy in a small area. These impellers are suitable for applications ranging from solid and gas dispersions and emulsification. Pressure impellers push against a static head while producing flow necessary to complete the process.

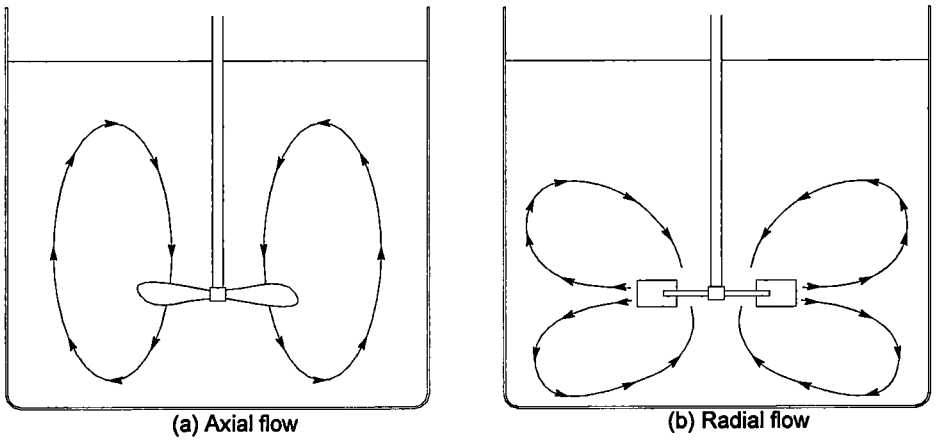

Figure 2.5 Examples of flow patterns.

Flow patterns in mixing vessels can generally be divided in three categories: axial, radial and tangential. Axial flow coincides with the axis of the impeller axis. When the impeller operates in a down-pumping mode, the flow impinges on the bottom of the tank and spreads out in all directions towards the walls. The flow rises upwards along the walls up to the surface and is pulled back to the impeller. This flow pattern is depicted in fig 2.5a. Axial flow impellers are the best impellers for producing flow. Because the flow does not take sharp turns near the impeller, power consumption of axial impellers is less compared to that of radial flow impellers at the same speed and with the same diameter.

Radial flow discharge is parallel to the impeller radius towards the vessel wall. If the impeller is not positioned close to the tank bottom or to the surface, the flow will split in two loops after impinging on the vessel wall. Each flow loop will continue along the wall and then return to the impeller. This flow pattern is depicted in see fig 2.5b. Radial flow is beneficial for high shear applications and increasing heat transfer.

Tangential flows are used in a much lesser extent. The tangential flow pattern is a swirling or vortexing flow in the rotation direction of the impeller. Tangential flow patterns offer very little mixing because the velocity gradients are very small. They can offer some advantages in heat transfer and in drawing down of solids, liquids or gasses from the liquid surface.

The natural tangential flow pattern tendency can be inhibited near the walls by using *baffles.* These are energy inefficient drag producers that are typically flat-stock metal beams or plates attached perpendicularly to the sidewalls of the tank. Power requirements are considerably

increased by the incorporation of baffles. A fully baffled tank usually has four baffles. Swirl is more pronounced with use of fewer baffles, baffles of less width or baffles set at an angle or mounted some distance away from the wall. Another way of inhibiting the tangential flow is to mount the agitator off-centre. This method is less suitable for radial flow type impellers. Mixing vessels must be designed in a way that stagnant zones are avoided. In a good vessel the tank, wall and bottom aid in directing the flow from the impeller. Sharp edges and steep cone bottom tanks must be avoided. Tank size and shape is most important in solids suspension applications because solids that settle in dead zones are extremely difficult do suspend.

As the Reynolds number decreases, the flow pattern of axial impellers approaches the flow pattern of radial impellers. In this regime the role of the baffles diminishes. All open impeller mixing systems exhibit a mix of radial and tangential flow patterns in the laminar zone. High viscosity fluids very often exhibit pseudoplastic behaviour. The viscosity of these fluids decreases with increasing shear rate. Because shear rates near the impeller are very high, the apparent viscosity near the impeller is low and depending on the rate of pseudoplastic behaviour. If the impeller diameter is too small compared to the vessel diameter (D/T), only the fluid in the impeller zone will rotate. To obtain sufficient bulk motion the impeller must cover a significant proportion of the vessel. The blades of the impeller may not be too narrow to prevent the impeller from slicing through the fluid. For good mixing of high viscosity pseudoplastic fluids impellers with wide blades and larger D/T are required.

A huge amount of different impellers with various geometries is available. A detailed description of all these types is beyond the scope of this report. Only a short description of frequently used types is given now. Some frequently used types are depicted in figure 2.6. Propellers, Rushton turbines, and high shear blades are generally used with relatively low viscosity systems and operate at high rotational speeds. Propellers are axial flow impellers where turbines and shear blades induce axial flow.

Anchors, helical ribbons and screws generally used for high viscosity liquids. The anchor and ribbon are arranged with a close clearance at the vessel wall. Kneaders Z-blade and sigma blade and Banbury mixers as shown are special mixing devices, generally used for mixing very high viscosity liquids, pastes, rubbers, etc.

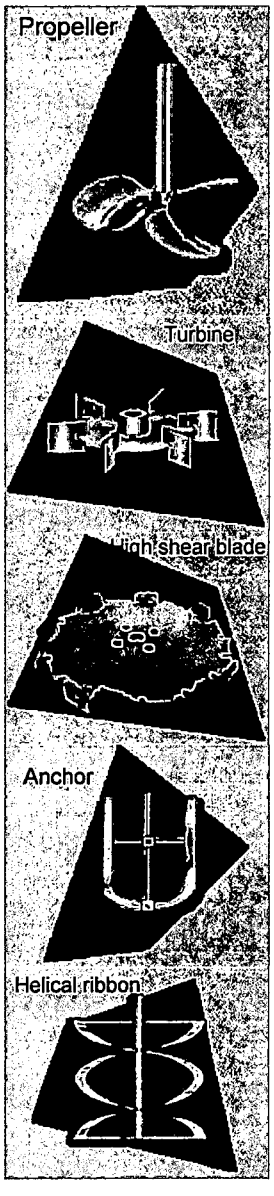

Figure 2.6 Common types of impellers

2.6.2 Extruders

Extruders are robust mixing devices normally used for mixing high viscous liquids. Mixing duties in the plastic industry are often carried out in either single or twin screw extruders. These units are usually fed with the base polymer in granular or powder form, together with additives. Flow in extruders is laminar. Shear results in an increase in interfacial area. Single screw extruders do not give good mixing. The mixing effect in a single screw extruder can be increased by means of mixing or shearing elements between or behind the screw flights, which induces crossing of streamlines.

Twin-screw extruders are usually classified into many types by their rotational direction and their intermeshing structure. These extruders may be co- or counter-rotary. Furthermore they can be non-intermeshing, partly intermeshing or closely intermeshing. Twin screw units can yield a product of better mixture quality than a single-screw machine. One of the problems is that a considerable amount of heat is generated and that the fluid properties may change by several orders of magnitude as a result of temperature changes. Especially for thermosetting materials, excessive heat generation is undesired. Mixing with extruders is described in detail in ref. 3.

2.6.3 Static mixer

Often used mixing devices for pipeline mixing are static mixers [ref.8]. Static mixers are also often used in the SMC production process to add the thickener component to the paste before the paste is transferred to the SMC machine (figure 1.1). One of the more common static mixer designs utilised today is the twisted ribbon type. This helical mixing element is mainly used for in-line blending of liquids under laminar flow conditions. Other types of static mixers are available for turbulent operating conditions.

The helical static mixer consists of a number of alternating right and left hand 180 degree helices. The elements are positioned such that the leading edge of an element is perpendicular to the trailing edge of the next element.

Mixing in the elements occurs through a combination of flow splitting and shearing at the junctions of successive elements and a stretching and folding within the elements. This process of splitting, stretching, folding and flipping repeats itself every two elements until the fluids are mixed. A computer simulation of the mixing of two liquids is depicted in figure 2.7.

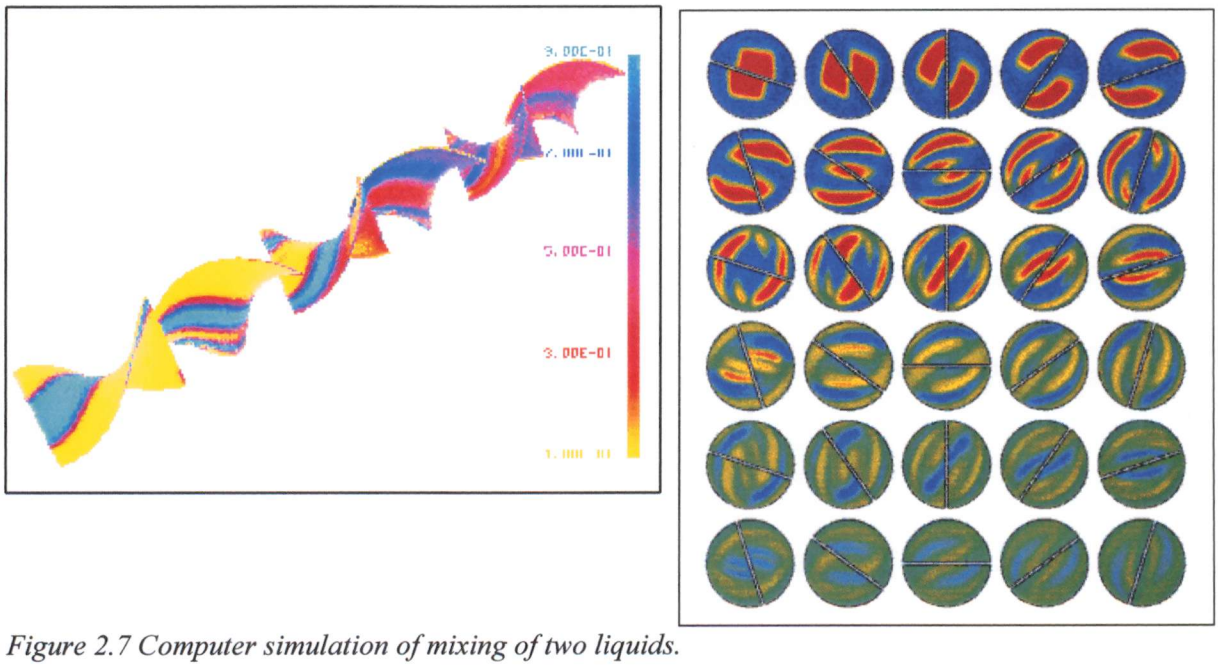

Figure 2.7 Computer simulation of mixing of two liquids.

2.7 Conclusions for paste preparation

The aim of this chapter is to find improvements for the mixing process of SMC paste. This paragraph describes theoretical requirements a mixing method for SMC paste must meet to obtain good homogeneity, good dispersion of the solid components, and high mixing efficiency to prevent excessive temperatures. The general mixing description of the previous sections is used to find improvements in the paste mixing process.

The mixing process of the paste can be divided in three parts. Usually the dilutions of unsaturated polyester resin and the thermoplastic resins are first mixed. These resins are diluted with styrene. Then the other liquid ingredients; styrene, solvents, initiator, accelerator, and inhibitor are added. This mixture of all liquid constituents is low viscous and Newtonian behaviour can be assumed [ref.1].

In the second phase of the paste preparation the solid releasing agent and filler powders are added to the batch after the liquid components are agitated for a sufficient time. The addition of the large amount of solid powders leads to a substantial viscosity rise. Also the rheologic behaviour changes into non-Newtonian. Finally the thickening agent is added in the third phase when the solid powders are well dispersed.

Usually the pastes are prepared in a mixing vessel. For all three phases only one impeller type is used. Sometimes a static mixer is used at production sites for the mixing of the thickener additive in the final phase.

Depending on the solubility of the liquid ingredients, the first phase of mixing process includes mixing of miscible liquids and mixing of immiscible liquids. In paragraph 2.4 is described that the mixing of two miscible phases requires high bulk fluid flow to ensure good contacting while generating very little shear that can emulsify the two components of the mix. If the resins and liquid additives are mixed with an impeller in a vessel, this type of mixing requires a flow inducing impeller that provides good contacting and top-to bottom motion throughout the vessel. Propeller mixers are suited for this purpose. Usually propellers are used with a diameter of one third of the vessel diameter.

Examples of immiscible liquids that are used in paste formulations are some LPA additives. An overview is given of the miscibility of several LPA additives in table 2.1. If the formulation contains immiscible components, one phase must be dispersed into the other. For effective dispersion, the hydrodynamic stresses must be large enough to overcome the surface tension that tends to return the droplets to a spherical shape. This requires high shear or intensive agitation. For this purpose, a high shear inducing impeller is suited. This type usually produces a radial flow pattern.

Resin	Miscibility
Saturated Polyester	single phase
Polyvinylacetate	single phase
Polymethyl methacrylate	two phase
Styrene/Butadiene triblock copolymer (rubber)	two phase
Polystyrene	two-phase

Table 2.1 miscibility of LPA resins

The solid components are added to the batch when all liquid components are homogeneously mixed. Usually the releasing agent is first mixed after which the filler is added. Addition of the solids leads to a change of the rheological behaviour of the mixture and to a rise of the apparent viscosity. The behaviour changes from Newtonian to pseudoplastic [ref.1][ref.6].

Effective dispersion of the solid powders requires high shear to induce rupture of agglomerates. The high energy input leads to a temperature rise of the mixture. This rise of temperature causes evaporation of styrene. To prevent excessive loss of styrene, usually the mixing is stopped when a temperature of 35°C is reached. For this reason efficiency of the dispersion process is very important. To obtain an efficient method to disperse the solids, all

material must be exposed to high shear as much as possible. To achieve this, the high shear zone must cover a large portion of the batch, or high shear and strong flow induction must be combined so that all material passes the high shear zone frequently. A twin-screw extruder is an example of a mixing device in which the high shear zone covers a large portion of the system.

The high shear zone is relatively small if the batch is mixed with an impeller in a vessel. An impeller with wide blades and a large diameter is required to obtain sufficient bulk motion because off the high apparent viscosity and the pseudoplastic behaviour. Only the fluid in the impeller zone will rotate if the impeller diameter is to small compared to the vessel diameter (D/T)

In section 2.6.1 is explained that impellers are available in different geometries that are categorised by their ability to dissipate energy in a combination of flow, shear and pressure. Either the flow component or the shear component can be emphasised. It might be necessary to use distinct devices for flow- and shear induction because it is difficult to combine high shear induction with a sufficient flow induction in one impeller. An example of a mixing configuration in which shear and flow are induced by distinct devices is depicted in figure 2.8. In this set-up a helical ribbon provides sufficient bulk motion where a high shear impeller takes care of the fragmentation of solids. For good dispersion a high tip speed (>8m/s) of the impeller is necessary. The helical ribbon needs a low speed of approximately 2 m/s. In the configuration of figure 2.8, the vessel rotates and the helical ribbon is fixed.

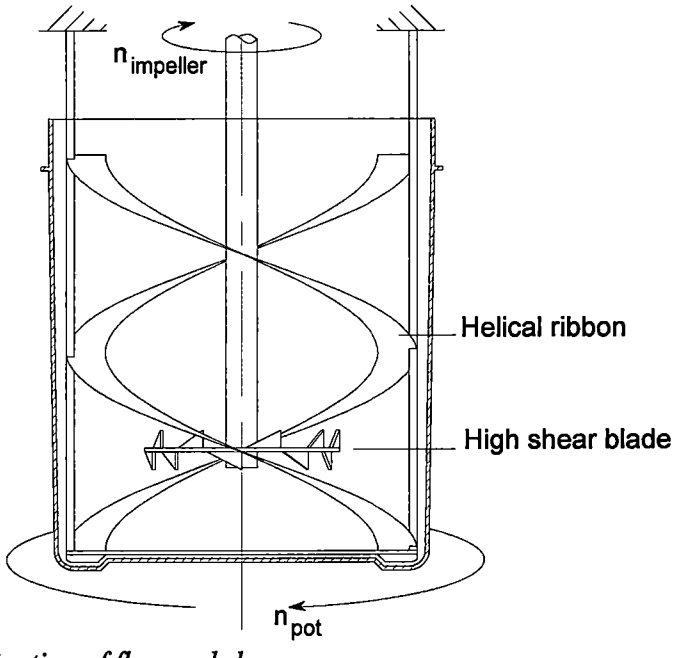

Figure 2.8 Combination of flow and shear.

The final step in the preparation of the paste is the addition of the thickening agent. Usually a predispersed MgO paste is used [section 1.2]. The addition of the thickener only implies mixing of the miscible MgO-paste into the batch because the MgO is already dispersed. For this, high bulk fluid flow is required to ensure good contacting. Little shear must be generated to prevent unnecessary temperature rise. The high shear impeller that was used in the second phase for dispersion of the solid powders is not suitable for this purpose. A propeller mixer with wide blades and a large diameter is needed for inducing the required bulk flow. This propeller can be combined with the helical ribbon depicted in figure 2.8 for optimal flow induction.

For good mixing in al phases of the paste preparation, it is important that stagnant regions and isolated mixing regions (IMR's) are avoided. To avoid stagnant zones, a vessel is used in

which the tank wall and bottom aid in directing the flow from the impeller. Moving the impeller to various heights in the vessel during mixing can destroy IMR's.

From the preceding can be concluded that the three phases of the paste preparation represent three different situations that need different types of mixing. The properties of the three phases with their mixing requirements are summarised below.

	Phase properties	Mixing requirements
Phase I	Mixing of low viscous miscible liquids. Newtonian behaviour can be assumed.	Requires high bulk flow to ensure good contacting. A propeller mixer is suitable for this purpose
	(Mixing of immiscible liquids)	Requires high shear or intensive agitation for dispersion. A high shear mixer can be used.
Phase II	Dispersion of solid powders. The apparent viscosity rises substantially. The rheologic behaviour changes from Newtonian to pseudoplastic.	Requires high shear for good dispersion. Also high bulk flow is required to so that all material passes the high shear zone frequently. It might be necessary to use distinct devices for flow- and shear induction.
Phase III	Mixing of the miscible MgO-paste into the high viscous pseudoplastic paste	Requires bulk flow. High efficiency is important to prevent unnecessary temperature rise. A propeller with wide blades and large diameter can be used.

Literature

1. Burns, R., *Polyester Molding Compounds*, Marcel Dekker Inc., New York, 1982.
2. Coulson, J.M. Richardson, J.F., *Chemical engineering*, Volume 1, fourth edition, 1990
3. Manas-Zloczower, I., Tadmor, Z. et al., *Mixing and compounding of polymers, Theory and practice,* Hanser publishers, Munich, Vienna New York, 1994
4. Niederkorn, T.C. , Ottino, J.M., 'Chaotic mixing of Shear-Thinning Fluids', *AIChE Journal*, Vol. 40, No. 11, 1994
5. Ottino, J.M. , DeRoussel, P. , et al., 'Mixing and dispersion of viscous liquids and powdered solids', Department of Chemical Engineering Northwestern University Evanston, *Advances in chemical engineering*, vol. 25, 1997, p 105-198
6. Scott, F.,'The effect of Zinc Stearates on the Rheology of Unsaturated Polyester Resin Molding Compounds', 41st Annual conference, Reinforced Plastics /Composites Institute, The Society of the Plastics Industry, Inc., Session 15-B January 27-31, 1986
7. Shenoy, A. V., *Rheology of Filled Polymer Systems*, Kluwer Academic Publishers, UK,1999

Internet

8. Bakker, A., Laminar Flow in Static Mixers with Helical Elements,"The Online Book" at http://www.bakker.org/cfm, 1998
9. Bresler, L., Shinbrot, T., et al., Department of Chemical Engineering Northwestern University, Evanston Illinois 60208, http://www.chemeng.nwu.edu/mixing/papers/IsolRegs/chemesci.html, 1995
10. Chemical processing's fluid flow annual, http://www.chemicalprocessing.com/protected/fluidflow/51.shtml
11. General process considerations for top entering agitators, http://www.proquipinc.com/process.html

3 Moulding of paste and SMC

3.1 Introduction

The aim of this chapter is to describe changes in rheological behaviour and volume during moulding of paste and SMC. Special attention is given to differences between paste and SMC behaviour. Good understanding of the moulding process is important because it will serve as basis for the modelling of shrinkage relations between pastes and SMC.

During processing of paste and SMC several profound changes take place in the rheological behaviour. After the paste is prepared, the thickening reaction causes an increase in elasticity of the system [paragraph 1.2]. During moulding the material is deformed and warmed up by the heated mould. Finally the material is changed from a viscoelastic fluid into a viscoelastic solid by a crosslinking reaction. The rheological behaviour is further complicated by the wide variety of contents used to modify the formulation. Each of these contents has an effect on the rheological response of the material. The difference in moulding behaviour of paste and SMC is caused by the fibre content. As described in paragraph 1.2, many variations are possible in for example the glass content, solubility of the sizing and the aspect ratio of the chopped strands.

Several types of test methods are available for examination of the behavioural changes during processing. Rheological behaviour of thickened paste and SMC can be illustrated with dynamic mechanical analysis, dielectric analysis and squeeze flow rheometry. For examination of the rheological behaviour of thickened paste the cappilary rheometer is also suited. For examination of the actual processes, occurring during moulding, an instrumented mould with temperature and pressure transducers on several places is very useful. The vertical movement of the mould during moulding can be monitored with displacement transducers. Furthermore the material flow can be examined with flow visualisation techniques.

In this chapter first a description is given of the various methods that are available for examining the behaviour of paste and SMC. In the following paragraphs the rheological behaviour will be discussed of thickening and thickened paste and SMC under isothermal conditions. Because the actual moulding is not an isothermal process, the influence of non-isothermal conditions on the flow in the mould is then described. Finally the actual processes occurring during moulding will be discussed.

3.2 Methods for examining behaviour of paste & SMC

3.2.1 Dynamic Mechanical Analysis

[ref.5.] [ref.8.] A common dynamic mechanical analysis (DMA) employs a sinusoidal forced torsional deformation with measurement of the resulting torque. The deformation is in shear and normally is limited to the linear viscoelastic region of the material response. From the deformation and the torque the stress and strain are calculated. If the material exhibits ideal elastic (Hookean) behaviour, the elastic response of the material is in phase with the applied strain.

$$\sigma(t) = \sigma_0 \sin(\omega t) = G\gamma_0 \sin(\omega t) \qquad (3.1)$$

If the material exhibits ideal viscous (Newtonian) behaviour, the stress is $\pi/2$ rad out of phase with the deformation.

$$\sigma(t) = \eta\frac{d\gamma}{dt} = \eta\gamma_0 \cos(\omega t) = \sigma_0 \sin(\omega t + \frac{\pi}{2}) \qquad (3.2)$$

The result of viscoelastic behaviour is that the strain lags the stress by a loss angle δ as presented in figure 3.1a. This can be represented as a resultant stress vector from the viscous loss and elastic storage contributions as depicted graphically in fig 3.1b.

$$\sigma(t) = \sigma_0 \sin(\omega t + \delta) = \sigma_0[\sin(\omega t)\cos\delta + \cos(\omega t)\sin\delta] \tag{3.3}$$

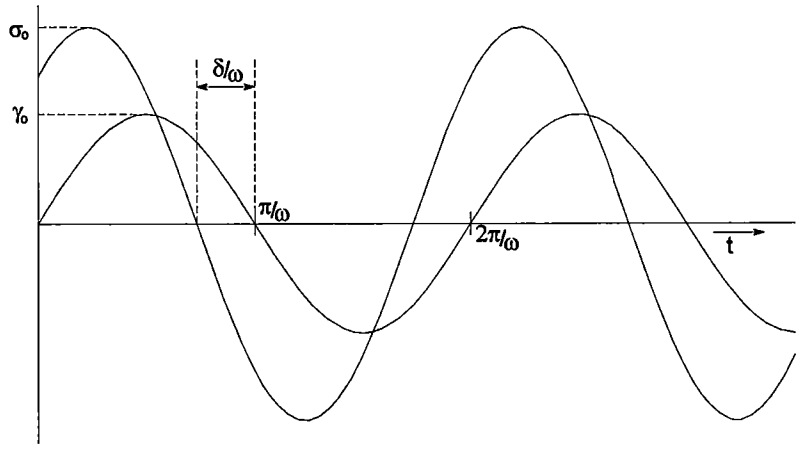

Figure 3.1a

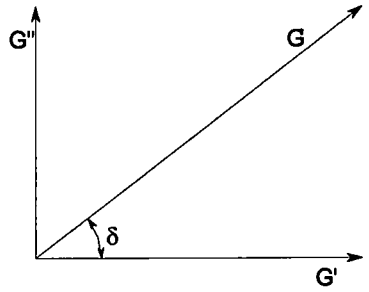

Figure 3.1b

By defining:

$$G' = \frac{\sigma_0}{\gamma_0}\cos\delta \text{ and } G'' = \frac{\sigma_0}{\gamma_0}\sin\delta \tag{3.4}$$

The stress may be written as:

$$\sigma(t) = \gamma_0[G' \sin(\omega t) + G'' \cos(\omega t)] \tag{3.5}$$

Where $\gamma_0 G' \sin(\omega t)$ is the elastic part of the stress and $\gamma_0 G'' \cos(\omega t)$ is the viscous part of the stress. The frequency dependent properties G' [Pa] and G'' [Pa] are the storage modulus and the loss modulus, respectively. The ratio of the plastic and the elastic component is the tangent of the loss angle.

$$\frac{G''}{G'} = \tan\delta \tag{3.6}$$

It follows that the complex modulus (G'') is a vector sum of the storage modulus and the loss modulus. Also a complex viscosity can be calculated.

$$G^* = \sqrt{G'^2 + G''^2} \tag{3.7}$$

$$\eta^* = \frac{G^*}{\omega} \tag{3.8}$$

The viscoelastic properties G', G'', $\tan\delta$, and η^* can be measured as function of frequency and temperature to study material properties, transitions and reactions. Rheological effects and chemical thickening progression of uncured paste and SMC can be examined by an

isothermal frequency sweep with fixed strain. G', G'', and η^* are calculated and plotted against frequency or strain rate. The reactivity and change in behaviour can be examined by using a fixed frequency and monitoring G', G'', and η^* during a rise of temperature.

For testing uncured paste or SMC the parallel plate geometry illustrated in fig 3.3 is the most suitable. Serrated plates are often used to prevent slip at the surface of the plates. Some shortcomings of the technique are volatilisation of the monomer and a non-uniform shear field with the parallel plate geometry.
With the assumptions of isothermal conditions, laminar flow, velocity only in angular direction, and negligible inertia and gravity, the following equations have been derived [ref.5.].

$$\tau = \frac{M}{2\pi R^3}\left[3 + \frac{\partial \ln M}{\partial \ln \dot{\gamma}_R}\right]$$

$$\gamma = \frac{\theta R}{h} \qquad (3.9)$$

$$G^* = \frac{\tau}{\gamma}$$

Where

τ = stress [N/m²]
M = torque [N·m]
R = radius of plate [m]
$\dot{\gamma}_R$ = shear rate at perimeter of plate [sec^{-1}]
γ = shear strain [-]
θ = angular deformation [rad]
h = gap height [m]

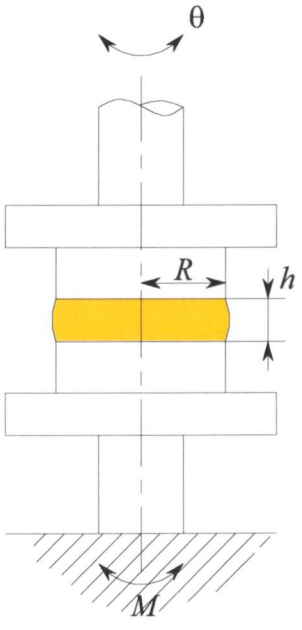

Figure 3.3 Parallel plate geometry

3.2.2 Dielectric testing

[ref.5.]
A very useful method for monitoring the effects of the chemical thickening reaction and the change in behaviour during curing is dielectric testing. In a dielectric cure measurement (DCM) a sample is imposed to an oscillating electrical field. Analogous to DMA, with DCM, the material response to the sinusoidal varied electrical field is measured. The oscillating electrical field tends to align the dipoles and ions in the material. Dipoles are molecules with a positive and a negative loaded side and ions. This results in dissipation of energy. The possibility of alignment depends on the mobility of the dipoles and ions. This is depicted schematically in figure 3.4. Depending on the mobility of the dipoles and ions, the induced voltage and the resultant current flow are out of phase. The phase angle decreases with increasing immobility. Measured quantities are the conductance G and the capacitance C. Information about the elastic and viscous components can be obtained by using the following equations:

$$\varepsilon' = \frac{G}{C_0 \omega}$$

$$\varepsilon'' = \frac{C}{C_0} \qquad (3.10)$$

$$\frac{\varepsilon'}{\varepsilon''} = \tan\delta$$

ε' = storage permittivity
This is a measure of elasticity of the rotating polymer chain segments.

ε'' = loss permittivity
This is a measure of frictional energy loss due to dipole rotation.

G = conductance

C = capacitance

C_0 = capacitance of air

ω = frequency of the applied field [rad/s]

δ = tangent of phase angle

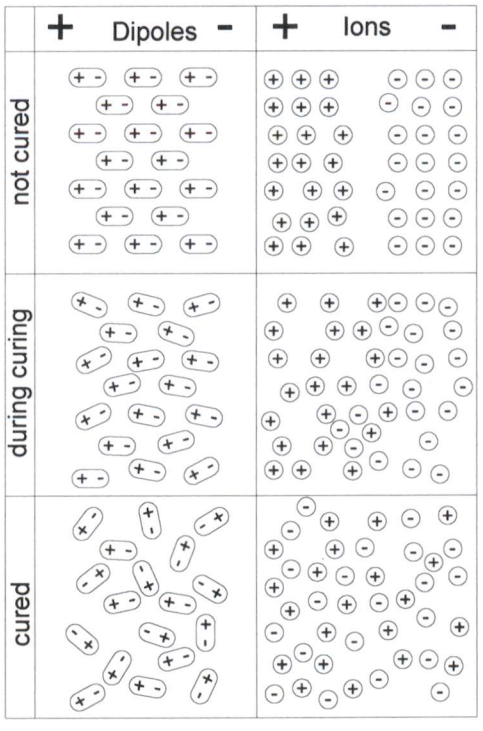

Figure 3.4 Dipoles alignments

The storage permittivity ε' is a measure of elasticity of the rotating polymer chain segments. The loss permittivity ε'' is a measure of frictional energy loss due to dipole rotation. The tangent of phase angle δ is analogous to the $\tan\delta$ in the DMA a measure for dampening

3.2.3 Squeeze flow measurement

[ref.1.][ref.5.] In a squeeze flow rheometer a precut specimen is squeezed at a constant velocity to a predetermined compression level while the resulting force is measured. By stopping the squeeze movement at a predetermined compression level, stress relaxation can be measured. In figure 3.5a the schematic geometry of a squeeze flow rheometer is presented.

The most convenient geometry is the open-ended parallel disk geometry. Because of the well-defined geometry, stress and shear rate can be calculated. A wide range of shear rates can be obtained by varying the closure velocity and sample thickness. The test can also be carried out at elevated temperatures.

3.2.4 Cappilary rheometer

Capillary rheometers are capable of extruding high viscous liquids through a capillary [ref.9.]. Therefore they are especially suited for examining the behaviour of thickened pastes. Capillary rheometers are broadly categorised as those operating at constant speed and those operating at constant pressure. The principal features are depicted schematically in figure 3.5b. A major advantage is that high shear rate levels can be achieved. The measurement can also be carried out at elevated temperatures.

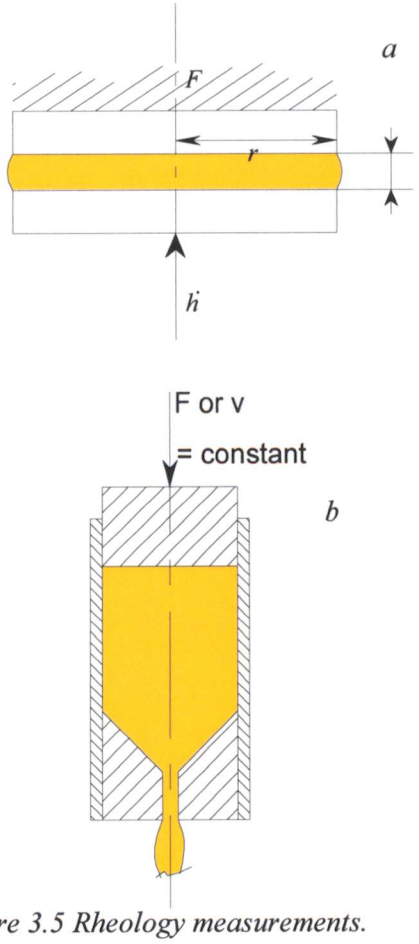

Figure 3.5 Rheology measurements.

3.2.5 Flow visualisation

[ref.3.] For obtaining a visual image of the flow behaviour during moulding, several techniques are available. Filling of the mould can be visualised with interrupted moulding experiments and video observation with transparent moulds.

Flow patterns can be visualised by moulding multicoloured charges of paste or SMC. The multicoloured charges can be obtained by assembling pigmented and not pigmented materials. Layered charges can be used for examination of flow patterns in the cross section of the charge. Chess patterns can be useful for examining flow in the plane of the product.

Because pigments can have profound influence on the material behaviour lead to changes in flow behaviour [Paragraph 1.2]. Therefore the pigment should only be used in very small amounts.

3.2.6 Instrumented mould

In order to understand the flow and curing behaviour of paste or SMC during moulding, an instrumented mould can be used. Temperature and pressure changes during moulding can be monitored using temperature and pressure transducers on several locations of the mould surface. Local pressure can be monitored with piezoelectric pressure transducers and temperatures can be measured with thermocouples that are thermally isolated from the mould. The vertical movement of the mould during moulding can be monitored with displacement transducers. An example of an instrumented mould is depicted schematically in figure 3.6.

The temperature measured with a thermocouple is a local value. The pressure on the other hand depends on the state of the charge. In low viscous state, the measured pressure is an average over a large volume. With increasing viscosity differences in pressure can occur over smaller distances. In solid state, the measured pressure is a local value. The output of the displacement measurement gives a measure of volume change during the moulding cycle. This value is the average over the entire charge.

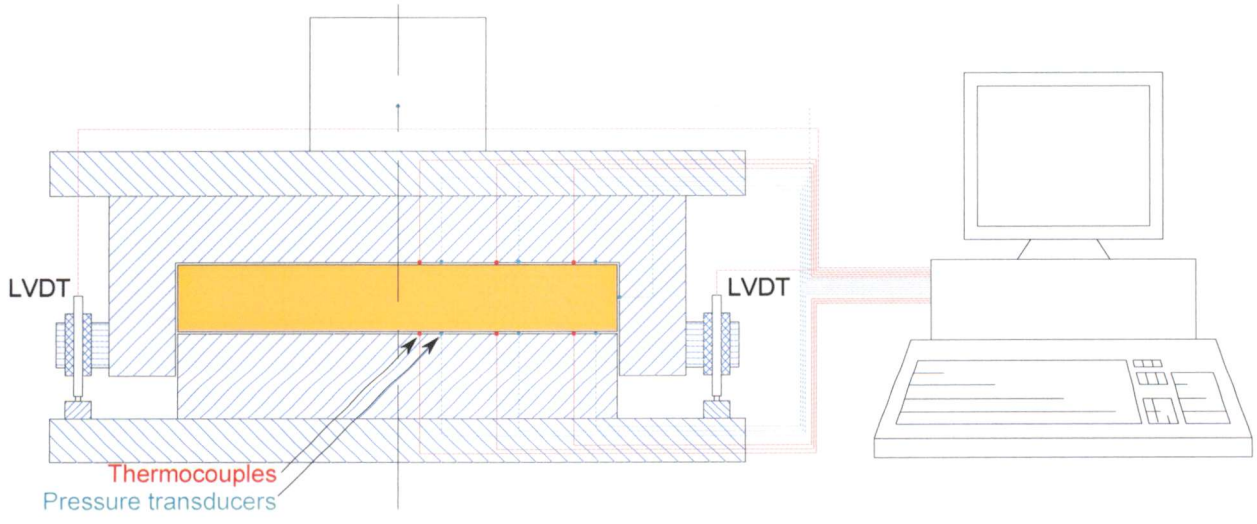

Figure 3.6 Example of instrumented mould.

3.3 Results for paste & SMC

3.3.1 Rheology during thickening

The final step in the preparation of paste is the addition of thickener. In the first few hours, minimal viscosity rise occurs. In case of SMC processing, glass fibres can be wetted in this time. Next the viscosity rises relatively fast. The rheological effects of the chemical thickening process can be examined using dynamic mechanical analysis (DMA). In figure 3.7 typical changes in the viscoelastic response of the material during the thickening are presented. [ref.5.]

Directly after addition of the thickener, the paste shows mostly viscous behaviour. This indicates that during a single cycle of oscillation the polymer molecules can rearrange freely. As the thickening process progresses, both the elastic component G' as the viscous component G" of the response rise. The elastic component rises at a higher rate. A plateau in the elastic response curve develops at higher frequencies. These observations can be explained with the thickening theory described in paragraph 1.2. In the first stage of the thickening process, the molecular weight increases as result of end to end linkage of polyester chains. Rearrangements require longer time, which results in longer relaxation times. The plateau in the G' curve may be caused by the formation of bridging networks that restrict molecular motions. [ref.5.]

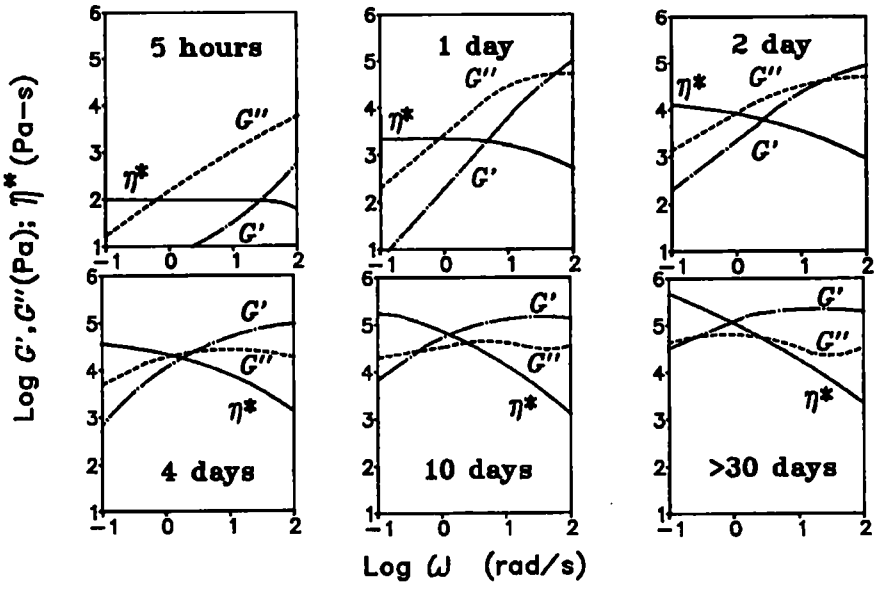

Figure 3.7 Rheological changes during chemical thickening.

3.3.2 Rheology of thickened paste

Rheological properties of the thickened paste have been examined with the capillary rheometer, DMA and squeeze flow tests. In examining the paste behaviour with the capillary rheometer various speeds and various temperatures were applied [ref.6.][ref.7.]. It was found that shear viscosities of the paste decrease with increasing shear rate, which indicates pseudoplastic behaviour. There is a high dependence of the viscosity on temperature. At low temperatures the material is highly non-Newtonian at all shear rates. At higher temperatures the Newtonian region extends to higher shear rates.

If previously extruded material was allowed to stand overnight and then recharged into the rheometer, the flow curves obtained are replicates of those obtained from original extrusion. This indicates that there is no shear breakdown in the material or the original structure is remade fairly rapidly [ref.7.].

Viscoelastic behaviour of the thickened paste can be examined with DMA analysis [ref.5.]. It is found that the thickened paste behaves like a viscoelastic fluid. The rheologic behaviour is strongly dependent on the mobility of the molecules. As thickening progresses the mobility decreases and relaxation times increase. Mobility is also strongly influenced by temperature and pressure. With increasing temperature, free volume increases and relaxation times decrease.

A typical squeeze flow curve for thickened paste is depicted in figure 3.8. The part of the curve with increasing stress consists of three parts. In the first part the material is compacted and locked air is eliminated. Then the material deforms elastically and the stress rises fast. Finally yield occurs and a steady state viscous flow is seen. After the squeezing is stopped, the stress relaxes in an exponential manner but does not return to zero. This relaxation curve is typical for a viscoelastic material.

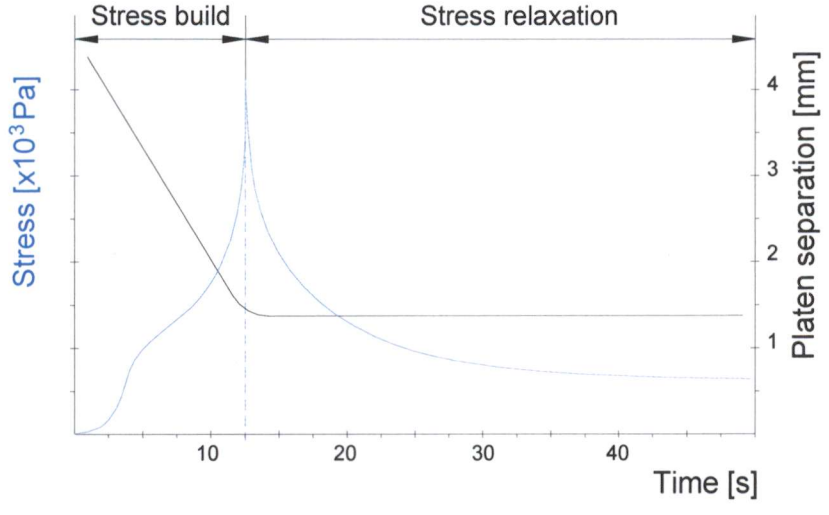

Figure 3.8 Squeeze curve of a paste.

With the assumptions of no slip at the wall, parabolic flow, and a significant pressure drop at edge of plates, the following equations for average shear stress, average shear rate at the wall and apparent viscosity have been derived. These assumptions are valid for the squeezing of paste but they are not for SMC.

$$\tau_w = \frac{F}{r^2}\frac{h}{r} \qquad \dot{\gamma}_w = \frac{3}{2}\frac{\dot{h}r}{h^2} \qquad \eta = \frac{\tau_w}{\dot{\gamma}_w} = \frac{2}{3}\frac{Fh^3}{\dot{h}\pi r^4} \tag{3.11}$$

Where:

F = force [N]
r = radius [m]
h = distance between plates [m]
$\dot{h}$ = closure velocity [m/s]
τ_w = average shear stress at the wall [N/m²]
$\dot{\gamma}_w$ = average shear rate at the wall [sec^{-1}]
η = apparent viscosity [Pas]

Stress relaxation of the paste follows modified Maxwell equation:

$$\frac{\tau_{(t)}}{\tau_{(0)}} = \left(\frac{t}{t_r}\right)^b \exp\left[-\left(\frac{t}{t_r}\right)^a\right] \tag{3.12}$$

Where:

$\tau_{(t)}$ = shear stress at time t [N/m²]
$\tau_{(0)}$ = shear stress at the onset of relaxation [N/m²]
t = time [s]
t = relaxation time constant [s]
a,b = fitting parameters [Pas]

As the velocity is increased, relaxation time constant t_r decreases and the final stress level after relaxation is lower. The increased closure velocity leads to more elastic behaviour because with higher rate of deformation the molecules have less of a chance to relax or release stress through viscous flow. [ref.1.]

3.3.3 Rheologic behaviour of uncured SMC

[ref.5.] The difference between paste and SMC is the incorporated glass. The rheological behaviour of the matrix still exists but the reinforcement has a strong effect on the material response. SMC consists of a viscoelastic matrix described in the previous paragraph with fibres acting as a supporting interacting network. When SMC is deformed at room temperature inhomogeneous flow occurs [ref.6.]. Under uniaxial extension, the fibres tend to segregate from each other and are pulled out from the resin at certain locations. Under simple shear the SMC behaves like a laminate consisting of many layers and it deforms like a deck of cards being slid. The extensional viscosity of an SMC is much larger than its shear viscosity. Adding glass fibres increases the extensional viscosity two decades or more, but the shear viscosity remains of the same order of magnitude [ref.6.].

The viscosity of an SMC compound is an apparent viscosity that characterises the flow resistance. On microscale the flow involves relative motions between fibres. Drag forces are generated on the paste between the fibres. The global extensional flow actually consists of many local shear flows.

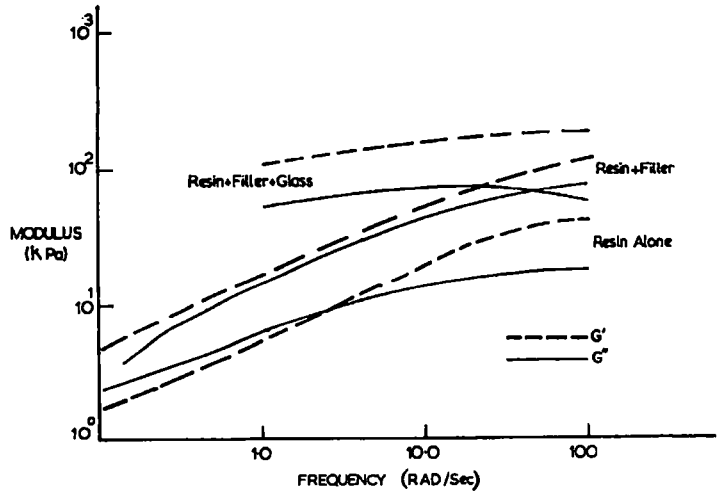

Figure 3.9 Effect of filler and glass fibres on G' and G".

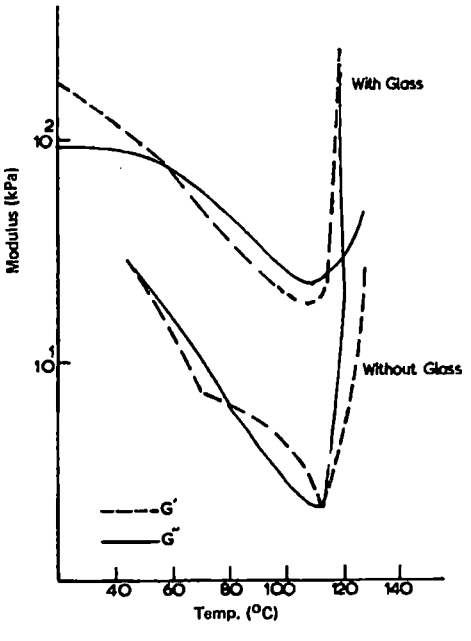

Figure 3.9b Effect of Temperature on G'and G"

In figure 3.9a the effect of glass content on G' and G'' obtained from a DMA analysis are depicted [ref.2.]. The figure shows that addition of glass fibres gives a sharp rise to both G' and G'' at the lower frequency ranges. The glass content reduces the response to frequency increase. At all frequencies the glass has a larger effect on the elastic component than it has on the viscous component. The effect of temperature on G' and G'' is depicted in figure 3.9b

for a paste and for SMC. The effect of the glass is a substantial increase in both the elastic and the viscous components. The sharp rise of the moduli above 100°C corresponds to the onset of curing.

Flow of SMC in the squeeze flow test has been studied in isothermal conditions at room temperature [ref.1.][ref.6.]. The isothermal experiments were conducted with both, lubricated and non-lubricated plate surfaces. The squeeze flow of SMC between lubricated plates is found to be a biaxial extensional flow. Without the lubrication the flow is more parabolic. The surface layers tend to stick to the wall and the centre layers have the maximum velocity. A typical squeeze flow curve for SMC is depicted in figure 3.10. Analogous to the paste squeeze curve, the part of the curve with increasing stress consists of three parts, compaction, stress build and yield [ref.1.]. An increase in fibre reinforcement loading leads to a more prevalent region of compaction because increased glass interactions and stacking can accommodate additional voids. Increasing the glass content also leads to higher stiffness resulting in higher stress levels.

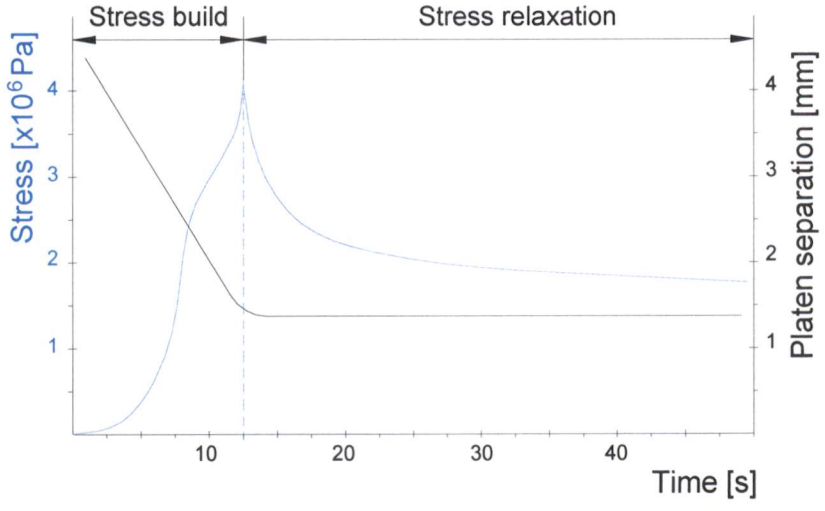

Figure 3.10 Typical squeeze curve for SMC.

Between lubricated plates, SMC exhibits biaxial extensional flow and is self-supporting in comparison to the paste. Therefore the assumptions of no slip at the wall, parabolic flow, and a significant pressure drop at edge of plates are not valid for SMC. With the assumption of an infinite plate and therefore no pressure drop, the following equations for average shear stress, average shear rate at the wall and apparent viscosity have been derived for SMC [ref.1.].

$$\tau_a = \frac{F}{\pi r^2} \qquad \dot{\gamma}_a = \frac{3}{2}\frac{\dot{h}r}{h^2} \qquad \eta = \frac{\tau_a}{\dot{\gamma}_a} = \frac{2}{3}\frac{Fh^3}{h\pi r^3} \tag{3.13}$$

Where:

F = force [N]
r = radius [m]
h = distance between plates [m]
$\dot{h}$ = closure velocity [m/s]
τ_a = apparent shear stress at the wall [N/m²]
$\dot{\gamma}_a$ = apparent shear rate at the wall [sec^{-1}]
η = apparent viscosity [Pas]

It has been found that squeeze flow viscosity data result in higher values than those measured with DMA. This is not surprising because extensional viscosities are higher than shear viscosities.

3.3.4 Non isothermal flow

With the actual moulding, a charge is squeezed between preheated moulds. This results in thermal gradients, both in the cross section of the charge and in the plane of the mould surfaces. Non-isothermal flow in a preheated mould is quite different from isothermal flow [ref.3.][ref.6.]. Material close to the mould surfaces is warmed up. Due to the temperature gradient normal to the mould surfaces a viscosity gradient develops which in turn leads to a velocity gradient near the surface.
The nature of non-isothermal flow of SMC in compression moulding has been examined with many moulding experiments. Flow patterns have been examined by assembling charges of materials with different colours [ref.3.]. Furthermore flow during moulding has been monitored using moulds instrumented with pressure-, temperature and mould displacement transducers.

Descriptions of non-isothermal paste flow experiments have not been found in literature. Probably because moulding of unreinforced pastes is not usual. First non-isothermal flow behaviour of SMC will be described. Then the flow of paste in non-isothermal conditions will be discussed.

With compression moulding of SMC, the mould is usually charged with 2-4 layers of SMC covering 30-70 percent of the mould surface. Usually very little mixing of the SMC-plies during moulding is observed [ref.5.]. During the mould closure, a lubricating resin rich layer develops at the surfaces of the moulds. The thickness of this surface film has been estimated to be approximately 15 to 25 μm.

In general the SMC flows in uniform extension through the thickness of each layer with slip at the mould surface. This is a consequence of the lubricating layer along the mould walls and the high modulus of the SMC. Because a thermal gradient exists in the cross section of the SMC charge, the warmer external layers tend to flow faster than colder interior layers. Between charging and closing the mould, some time passes, resulting in a small temperature difference between the upper and lower layers. This leads to slightly more flow of the lower layers. SMC apparent viscosity, the rate of heat transfer and mould closing speed have great influence on the flow pattern. At rapid closing speed, the entire charge extends uniformly through its thickness with slip concentrated at the mould surface. For lower closing speeds on thicker charges also slip occurs between the outer SMC layers. Typical flow patterns for normal closure rates are shown in figure 3.11.

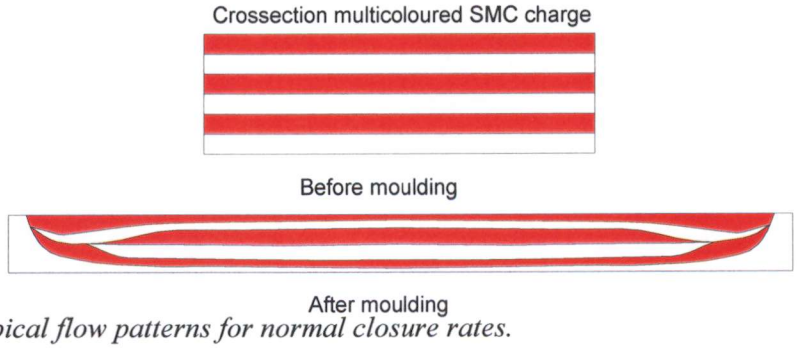

Figure 3.11 Typical flow patterns for normal closure rates.

The thermal gradient in the cross section of the charge causes hot low viscous external material to flow away from the centre to the edges of the mould. This results in a thermal gradient in the X-Y plane of the charge. Furthermore a thermal gradient is established in the mould itself. Where the charge is placed on the heated moulds, heat transfer occurs in the initial charge area, causing a reduction in mould temperature at that point. The heat is pumped to the edges by the warm material flow resulting in lower mould temperatures in the charge area and higher mould temperatures at the edges of the mould.

There are several differences between the moulding of paste and SMC. An important difference is that contrary to SMC, paste exhibits low resistance to extensional deformation

due to the absence of the glass fibre reinforcement. Furthermore the thickened paste is charged as one continuous block instead of a stack of thin plies. The paste charge usually has a larger thickness and covers a smaller initial area of the mould surface.

When paste is moulded, as with SMC-moulding, probably a low viscous lubricating layer will develop at the surfaces of the moulds. A thermal gradient will exist in the cross section of the charge, and the warmer external material will tend to flow faster than colder interior material. Due to the large thickness of the paste charge, this temperature gradient will only exist in a relatively small area near the walls.

With the closing of the mould the difference in resistance against deformation will lead to a big difference in ram force during the squeezing. This leads to a lower driving force for squeezing out of low viscous material compared to an SMC moulding. Probably the creation of a thin low viscous lubricating layer, the low resistance against extension, the low driving force for inhomogeneous flow and the relative homogeneous temperature distribution through thickness will lead to a homogeneous lubricated extensional flow of the paste during the closure of the mould.

3.3.5 Rheological- and volumetric changes during curing

As explained in chapter 1.2 the unsaturated polyesters cure by free-radical copolymerisation between unsaturated bonds in the polyester chains and monomeric styrene. During the curing reaction a substantial change of the material characteristics is observed. The material transforms from a viscoelastic liquid to a viscoelastic solid. Furthermore the volume of the material changes during curing [ref.4.].

There are several ways to monitor the progress of the curing reaction. Because the curing is an exothermal reaction, it can be monitored by measuring the rate of heat release. Heat release can be measured in a differential scanning calorimeter (DSC). The amount of cure is usually taken as a measure for the degree of cure. The degree of cure can be defined as the fraction conversion c:

$$c = \frac{Q}{Q_T} \qquad (3.14)$$

Q = heat released up to current time
Q_T = total heat of reaction

Rheological changes during curing can be examined with DMA and DCM. Another valuable tool for examining the curing process is the mould instrumented with temperature-, pressure-, and mould displacement transducers. Measurements of DMA, DCM are conducted on very small amounts of material. When dimensions of the curing batch are small, the surface to volume ratio is large. This results in homogeneous warming up and small temperature gradients. In the actual moulding process, temperature gradients develop in thickness direction of the charge and in the XY-plane as described in the previous paragraph 3.3.4. Due to the thermal gradients, curing does not occur homogeneously but starts at locations with material of highest temperature and progresses to the material of lower temperature. In this paragraph first curing is discussed, assuming it is homogeneous curing. Then the inhomogeneous curing is described.

A typical heat versus time curve of isothermal curing behaviour is depicted in figure 3.12a [ref.6.]. It can be seen that the total curing can be divided in three periods. In the period before curing (precure period) no appreciable curing takes place due to the inhibitor [paragraph 1.2]. Then in the cure period, the curing first starts slowly, then accelerates and proceeds rapidly. Finally the reaction slows down because the crosslinking reaction inhibits molecular motions which bring reactants together. In the post cure period no appreciable curing takes place anymore.
A temperature-time curve of a curing cycle is depicted in figure 3.12b. In the precure period first an initial temperature rise due to heat conduction is visible. Then when the curing reaction

starts, a temperature transient due to the exothermic crosslinking reaction is visible followed by gradual cooling in the period after curing (post-cure period).

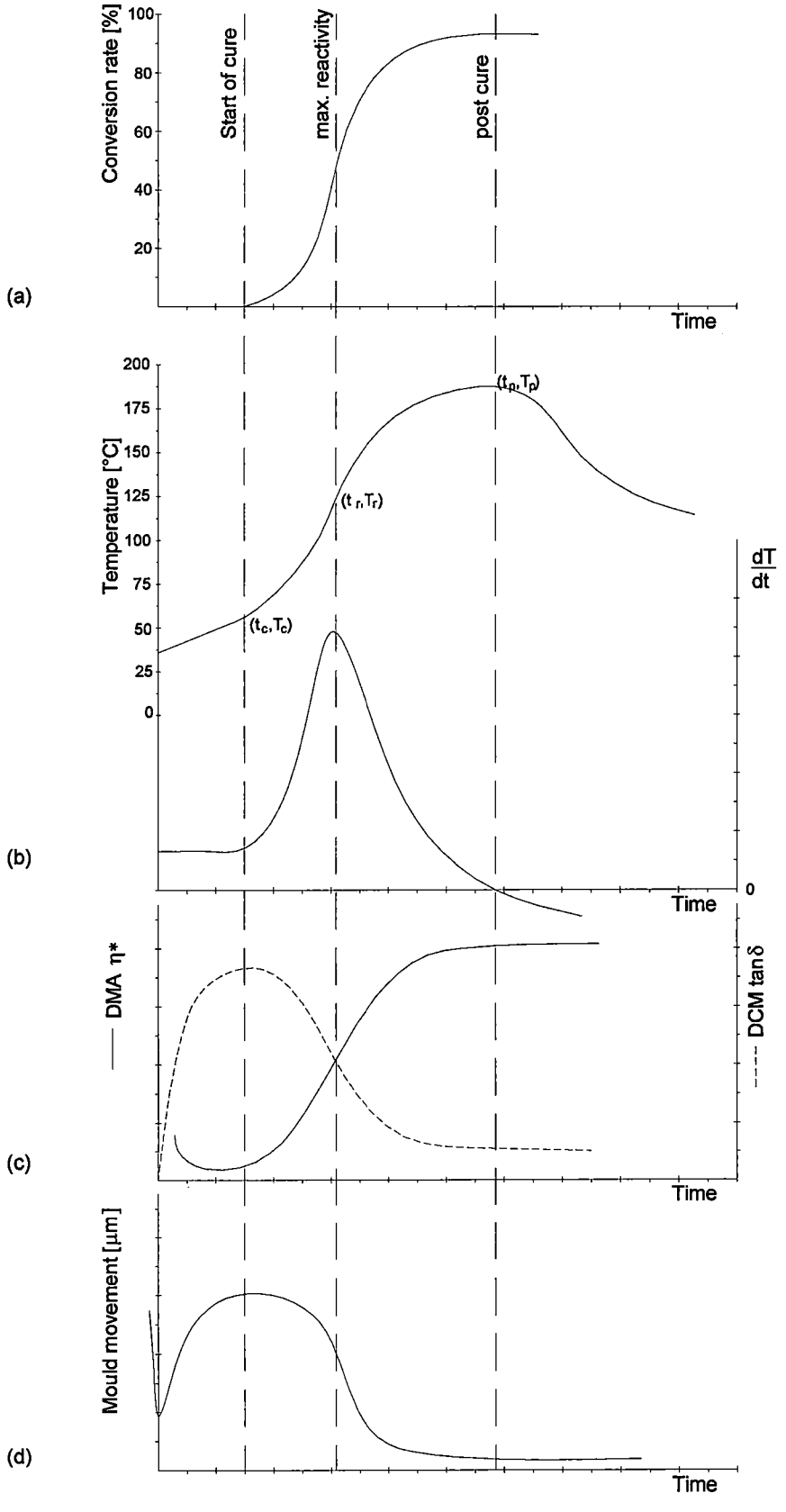

Figure 3.12 Rheological and volumetric changes during curing.

The crosslinking reaction can be accurately analysed by taking the derivative of the temperature-time curve. The cure reaction starts where the curve changes from a low constant dT/dt value to an increasing value. The derivative curve has a peak at co-ordinate (t_r, T_r). The height of this peak may be associated with the reactivity of the curing material. The location where dT/dt= 0 is indicates the end of reaction. A useful set of parameters can be derived to characterise the cure properties of a paste [ref.4.].

t_c	= precure time
t_p	= time to peak exotherm
$\delta t=t_p-t_c$	= reaction time
T_c	= onset reaction temperature
T_p	= peak exotherm
$\delta T=T_p-T_c$	= exothermic temperature rise associated with the reactivity of the paste

In figure 3.12c typical results are plotted of the DMA- and DCM output during curing [ref.5.]. In the precure period the dielectric response first increases with increasing temperature of the charge. This increase is caused by the increasing mobility of ions and dipoles due to the decrease of viscosity with rising temperature. This drop in apparent viscosity is visible in the DMA-curve. The peek in the tanδ corresponds to the time when the network is being formed. Then the DCM-curve declines and reaches a steady state, which indicates the material has become a glassy solid. A simultaneous rise leading to a plateau can be seen in the apparent viscosity. The peak in the tanδ lags the onset of the increase of the apparent viscosity because during the first part of the reaction, ionic mobilities are not restricted although the viscosity is increasing [ref.5.].

The mechanical response of the material during the curing cycle can be measured with the pressure- and displacement transducers. In figure 3.12d a typical is depicted. As mentioned before in paragraph 3.2.6, this curves is generated by averaging over a larger volume, in contrast to the temperature-time curve represents a point value. The pressure and mould displacements are closely related to each other because the pressure is the driving force of the mould displacement. Usually during a moulding cycle, the press system is programmed to generate constant moulding force. Nevertheless throughout much of the curing, the state of pressure in the paste differs from the set pressure due to interactions between the material and the press system. The pressure response is not only complementary to volume change but is also modulated by the press dynamics [ref. 4.].

First a rapid decrease in platen separation is visible in figure 3.12d during the closing of the mould. Subsequently the curve rises due to thermal expansion throughout the precure period, and levels off exponentially. After the onset of the crosslinking reaction, the displacement curve begins to decline due to shrinkage of the curing material. This shrinkage is referred to as polymerisation shrinkage. This shrinkage occurs in spite of the further increase of the temperature in the material. During the postcure period the material continues to contract at a slow rate because of a thermal shrinkage of the cured material cooling down from the peak exothermic temperature back to the mould temperature.

During the moulding cycle, the volume change of the material is influenced by several factors. First with the closing of the mould, the material is compressed by the moulding pressure (p). In the precure period the thickened viscoelastic material is warmed up. It changes into a viscoelastic liquid with low apparent viscosity. Relaxation times in this phase are very short. The changes of volume (V) are caused by the rising temperature (T) and the pressure (p).

$$dV_{\Pr ecure} = \left(\frac{\partial V}{\partial p}\right)dp + \left(\frac{\partial V}{\partial T}\right)dT \qquad (3.15)$$

In the formula, $\partial V/\partial p$ is the compression modulus and $\partial V/\partial T$ is the thermal expansion coefficient of the uncured material. During this part of the moulding, a hydrostatic state of stress can be assumed. The mould is completely filled. The volume change can be calculated from the mould displacement (δh) and the mould surface (A).

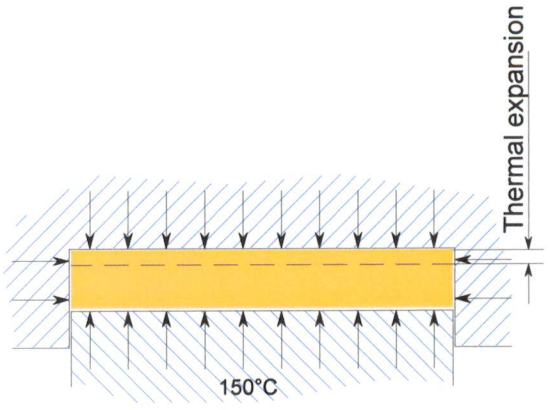

$$\delta V = A \cdot \delta h \qquad (3.16)$$

In the curing period the material changes from a low viscous viscoelastic liquid into a viscoelastic solid. Volume changes during the curing period are caused by changes in pressure (p) and thermal expansion due to the exothermal temperature rise. Furthermore volume changes due to the polymerisation shrinkage and LPA effects conversion (X) effects [ref.4.].

$$dV_{cure} = \left(\frac{\partial V}{\partial p}\right)dp + \left(\frac{\partial V}{\partial T}\right)dT + \left(\frac{\partial V}{\partial X}\right)dX \qquad (3.17)$$

Because the shrinkage and transformation to a viscoelastic solid material occur during the curing period, the state of stress changes to non-hydrostatic. Under the non-hydrostatic conditions creep deformation of the viscoelastic material can occur. Also flow of uncured material can occur on locations where the cured material draws back from the mould edges.

In the post cure period, the material has turned into a viscoelastic solid. Thermal shrinkage occurs due to the cooling down to the wall temperature. Volume changes can be caused by pressure and temperature changes. The thermal expansion coefficient of the cured material in the post cure period is markedly different from that of the viscous material in the precure period. [ref.4.]. The thermal expansion coefficient of the material in the precure period is estimated to be $180 \cdot 10^{-6} K^{-1}$. In the postcure period, the thermal expansion coefficient of the solid material is reduced to approximately $55 \cdot 10^{-6} K^{-1}$ [ref.4.].

$$dV_{Postcure} = \left(\frac{\partial V}{\partial p}\right)dp + \left(\frac{\partial V}{\partial T}\right)dT \qquad (3.18)$$

[ref.7.] In the actual moulding, curing does not occur homogeneously due to the thermal gradients. The curing starts at locations with material of highest temperature and progresses to locations with material of lower temperature. In paragraph 3.3.4 is described that temperature gradients develop in thickness direction and in the XY-plane of the charge. Near the edges of mould the temperature is the highest. The curing reaction starts at the edges and propagates towards the centre of the mould. When the curing starts, the pressure drops near the mould edges due to polymerisation shrinkage. Simultaneously the pressure at centre of mould rises.

Flow of uncured low viscous material will occur from areas of high pressure to low pressure areas. As curing propagates, the area of low pressure propagates towards the centre of the mould. At end of cure, highest pressure is at the edge of the mould. This results in higher density at the edges of the plate

After the moulding cycle is finished, the mould opens and the plate is removed from the mould. The decompression will lead to an instant elastic relaxation and a time dependent viscoelastic relaxation. Also thermal shrinkage occurs due to the cool down to room temperature, figure 3.13. Experiments have also shown that after the plate is removed from the mould, still LPA's effect the shrinkage.

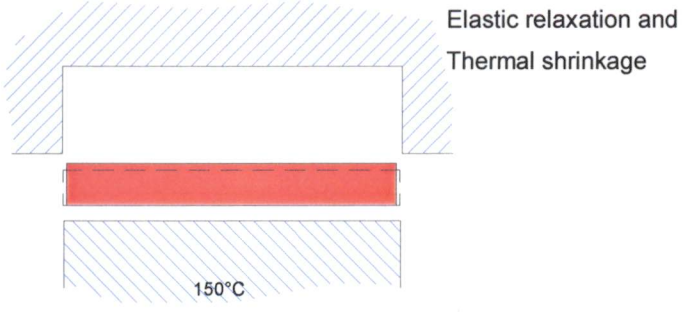

Figure 3.13 Volumetric changes after decompression.

Literature

1. Allen, P., Yeh, J.D., et al., 'Experimental Study of SMC Rheology using compression techniques', *SPI Composites Institute 45th Annual Conference 1990, Premix Inc.* , Akron University, Washinton 1990, paper 11-B, pp.6.627
2. Burns, R., *Polyester Molding Compounds*, Marcel Dekker Inc., New York ,1982.
3. Barone, M.R., Caulk, D.A., 'A model for the flow of a chopped fiber reinforced polymer compound in compression moulding', *Journal of Applied Mechanics*, Vol. 53/361, June 1986
4. Kau, H-T., 'An experimental study of the dynamics of the curing process of sheet molding compound paste', *Polymer Engineering and Science*, Vol. 29, No. 18, September 1998
5. Kia, H.G., *Sheet Molding Compounds, Science and Technology*, Hanser Publishers, 1993
6. Lee, L.J. Marker, L.F., et al., 'The rheology and mold flow of polyester sheet moulding compound', *Plastics ABCs Polymer Alloys, Blends&Composites; National Technical Conference,* Bal Harbour, 1982
7. Marker, L., Ford, B.W., 'Rheology and Molding characteristics of glass fiber reinforced sheet moulding compounds', *32nd Annual Technical Conference,* SPI, 1977
8. Nijenhuis, K. te, *Viscoelasticity, a short introduction*, Delft University of Technology , Delft, 1996
9. Aroon, V., Shenoy, *Rheology of filled polymer systems*, Kluwer Academic Publishers, 1999

4 Mechanics of composite materials

4.1 Introduction

This chapter describes the theory that is important for the calculation of SMC shrinkage properties and mechanical properties from measured paste properties. SMC's are composites cured paste material with random oriented short fibres. During and after the moulding of an SMC, temperature change, polymerisation shrinkage and LPA effects cause volume changes of the matrix. Also the fibre volume changes due to thermal effects. The theory of mechanics of composites is used to derive the necessary formulas for calculation of theoretical relations between paste and SMC. This theory is used in the final report for calculation of SMC properties from measured matrix properties.

The mechanical behaviour of an anisotropic material is first described. Paragraph 4.3 describes how the mechanical properties of the anisotropic composite material can be predicted from the properties of the constituents. How the expansion of the anisotropic composite material can be predicted from the properties of the constituents is explained in paragraph 4.4. In paragraphs 4.5 and 4.6 is explained how the stress-strain behaviour and the residual expansion can be predicted of laminates that consist of unidirectional plies with fibres oriented in various directions. Finally the theory is applied on Sheet Moulding Compounds in paragraph 4.7.

4.2 Stress-train relation of an anisotropic material

In case of linear elastic behaviour, the stress-train relation of an anisotropic material can be described with the generalised Hookes law. This relation describes the relation between six independent stress components and six independent deformation components that determine the state of stress and deformation of the material. Hooke's law in matrix notation is depicted below:

$$\sigma = C\varepsilon$$

$$\begin{pmatrix}\sigma_1\\ \sigma_2\\ \sigma_3\\ \sigma_4\\ \sigma_5\\ \sigma_6\end{pmatrix} = \begin{pmatrix}C_{11} & C_{12} & C_{13} & C_{14} & C_{15} & C_{16}\\ C_{21} & C_{22} & C_{23} & C_{24} & C_{25} & C_{26}\\ C_{31} & C_{32} & C_{33} & C_{34} & C_{35} & C_{36}\\ C_{41} & C_{42} & C_{43} & C_{44} & C_{45} & C_{46}\\ C_{51} & C_{52} & C_{53} & C_{54} & C_{55} & C_{56}\\ C_{61} & C_{62} & C_{63} & C_{64} & C_{65} & C_{66}\end{pmatrix}\begin{pmatrix}\varepsilon_1\\ \varepsilon_2\\ \varepsilon_3\\ \varepsilon_4\\ \varepsilon_5\\ \varepsilon_6\end{pmatrix} \qquad (4.1)$$

The matrix C is called the stiffness matrix. For the subscripts the contracted notation is used. Contracted notation is a simplification of the conventional notation (figure 4.1). The meaning of the indices is as follows:

$$\sigma_1 = \sigma_x \;;\; \sigma_2 = \sigma_y \;;\; \sigma_3 = \sigma_z \;;\; \sigma_4 = \tau_{yz} \;;\; \sigma_5 = \tau_{zx} \;;\; \sigma_6 = \tau_{xy} \qquad (4.2)$$

$$\varepsilon_1 = \varepsilon_x \;;\; \varepsilon_2 = \varepsilon_y \;;\; \varepsilon_3 = \varepsilon_z \;;\; \varepsilon_4 = \gamma_{yz} \;;\; \varepsilon_5 = \gamma_{zx} \;;\; \varepsilon_6 = \gamma_{xy}$$

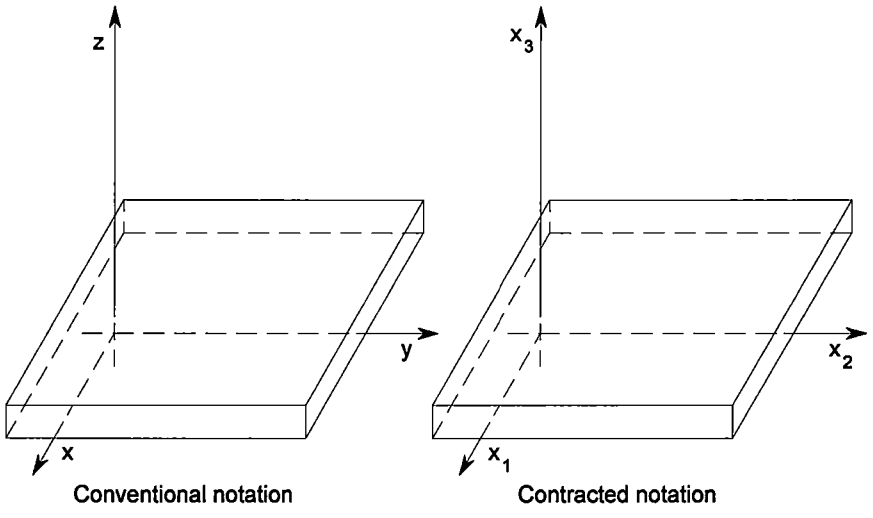

Figure 4.1 Conventional notation.

The deformation components can also be expressed as function of the stress components:

$$\varepsilon = C^{-1}\,\sigma = S\,\sigma \tag{4.3}$$

The matrix S is called the compliance matrix. The stiffness- and the compliance matrix are symmetric [Maxwell].

If a material has three mutual perpendicular planes of symmetry in each point, it is called orthotropic. The three intersection lines of these planes are the principal directions of the material. The stiffness- and the compliance matrix of an orthotropic material related to its principal directions are depicted below.

$$C = \begin{pmatrix} C_{11} & C_{12} & C_{13} & 0 & 0 & 0 \\ & C_{22} & C_{23} & 0 & 0 & 0 \\ & & C_{33} & 0 & 0 & 0 \\ & & & C_{44} & 0 & 0 \\ & & & & C_{55} & 0 \\ & & & & & C_{66} \end{pmatrix} \qquad S = \begin{pmatrix} S_{11} & S_{12} & S_{13} & 0 & 0 & 0 \\ & S_{22} & S_{23} & 0 & 0 & 0 \\ & & S_{33} & 0 & 0 & 0 \\ & & & S_{44} & 0 & 0 \\ & & & & S_{55} & 0 \\ & & & & & S_{66} \end{pmatrix} \tag{4.4}$$

The compliance matrix can also be expressed in engineering constants. The engineering constants of an anisotropic material are defined as follows:

Young's moduli

$$E_k = \frac{\sigma_k}{{}^{k}\varepsilon_k} = \frac{1}{S_{kk}} \tag{4.5}$$

Shear moduli

$$G_{23} = \frac{\sigma_4}{{}^{4}\varepsilon_4} = \frac{1}{S_{44}} \qquad G_{31} = \frac{\sigma_5}{{}^{5}\varepsilon_5} = \frac{1}{S_{55}} \qquad G_{12} = \frac{\sigma_6}{{}^{6}\varepsilon_6} = \frac{1}{S_{66}} \tag{4.6}$$

Poissons ratios

$$\nu_{kl} = -\frac{{}^{k}\varepsilon_l}{{}^{k}\varepsilon_k} = -\frac{S_{lk}}{S_{kk}} \qquad k,l \in \{1,2,3\} \tag{4.7}$$

In these definitions, ${}^{k}\varepsilon_l$ stands for the strain ε_l caused by the stress σ_k.
The compliance matrix of an orthotropic material can be expressed in the engineering constants as follows:

$$S = \begin{pmatrix} \frac{1}{E_1} & -\frac{\nu_{21}}{E_2} & -\frac{\nu_{31}}{E_3} & 0 & 0 & 0 \\ & \frac{1}{E_2} & -\frac{\nu_{32}}{E_3} & 0 & 0 & 0 \\ & & \frac{1}{E_3} & 0 & 0 & 0 \\ & & & \frac{1}{G_{23}} & 0 & 0 \\ & & & & \frac{1}{G_{31}} & 0 \\ & & & & & \frac{1}{G_{12}} \end{pmatrix} \tag{4.8}$$

If plane stress can be assumed, Hooks law can be reduced to:

$$\sigma = Q\varepsilon \qquad \varepsilon = Q\sigma$$

$$\begin{pmatrix} \sigma_1 \\ \sigma_2 \\ \sigma_6 \end{pmatrix} = \begin{pmatrix} Q_{11} & Q_{12} & Q_{16} \\ Q_{21} & Q_{22} & Q_{26} \\ Q_{61} & Q_{62} & Q_{66} \end{pmatrix} \begin{pmatrix} \varepsilon_1 \\ \varepsilon_2 \\ \varepsilon_6 \end{pmatrix} \qquad \begin{pmatrix} \varepsilon_1 \\ \varepsilon_2 \\ \varepsilon_6 \end{pmatrix} = \begin{pmatrix} S_{11} & S_{12} & S_{16} \\ S_{21} & S_{22} & S_{26} \\ S_{61} & S_{62} & S_{66} \end{pmatrix} \begin{pmatrix} \sigma_1 \\ \sigma_2 \\ \sigma_6 \end{pmatrix} \tag{4.9}$$

The constants Q_{ij} are the reduced stiffness constants. For an orthotropic material, the reduced stiffness matrix Q related to its principal directions, can be expressed in the engineering constants as follows:

$$Q = \begin{pmatrix} \frac{E_1}{1-\nu_{12}\nu_{21}} & \frac{\nu_{12}E_2}{1-\nu_{12}\nu_{21}} & 0 \\ & \frac{E_2}{1-\nu_{12}\nu_{21}} & 0 \\ & & G_{12} \end{pmatrix} \qquad S = \begin{pmatrix} \frac{1}{E_1} & -\frac{\nu_{21}}{E_2} & 0 \\ & \frac{1}{E_2} & 0 \\ & & \frac{1}{G_{12}} \end{pmatrix} \tag{4.10}$$

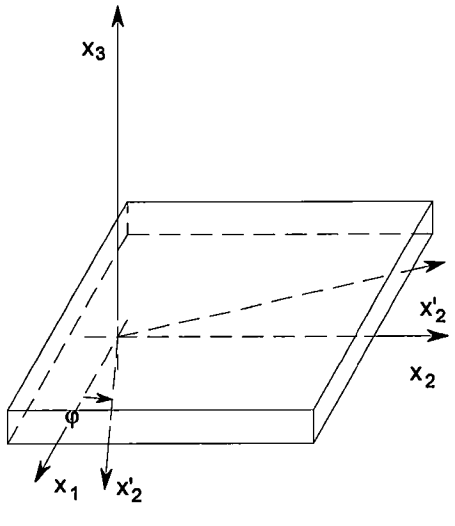

Figure 4.2 Transformation rotation in the 1-2.

To determine the mechanical properties of the composite in directions different from the principal directions, a transformation rotation in the 1 2-plane can be applied as depicted in figure 4.2. Stresses and strains can be transformed with:

$$\sigma' = T\sigma$$

$$\begin{pmatrix}\sigma_1'\\ \sigma_2'\\ \sigma_6'\end{pmatrix} = \begin{pmatrix}\cos^2\varphi & \sin^2\varphi & 2\sin\varphi\cos\varphi\\ \sin^2\varphi & \cos^2\varphi & -2\sin\varphi\cos\varphi\\ -\sin\varphi\cos\varphi & \sin\varphi\cos\varphi & \cos^2\varphi-\sin^2\varphi\end{pmatrix}\begin{pmatrix}\sigma_1\\ \sigma_2\\ \sigma_6\end{pmatrix} \qquad (4.11)$$

$$\varepsilon' = T^{-T}\varepsilon$$

$$\begin{pmatrix}\varepsilon_1'\\ \varepsilon_2'\\ \varepsilon_6'\end{pmatrix} = \begin{pmatrix}\cos^2\varphi & \sin^2\varphi & -\sin\varphi\cos\varphi\\ \sin^2\varphi & \cos^2\varphi & \sin\varphi\cos\varphi\\ 2\sin\varphi\cos\varphi & -2\sin\varphi\cos\varphi & \cos^2\varphi-\sin^2\varphi\end{pmatrix}\begin{pmatrix}\varepsilon_1\\ \varepsilon_2\\ \varepsilon_6\end{pmatrix} \qquad (4.12)$$

The reduced stiffness constants Q'_{ij} of an orthotropic material under plane stress conditions, after a transformation rotation over φ as depicted in figure 4.2, can be calculated from its reduced stiffness constants Q_{ij} related to its principal directions with:

$$\begin{aligned}
Q_{11}' &= \tfrac{1}{8}(3Q_{11}+3Q_{22}+2Q_{12}+4Q_{66})+\tfrac{1}{2}(Q_{11}-Q_{22})\cos 2\varphi+\tfrac{1}{8}(Q_{11}+Q_{22}-2Q_{12}-4Q_{66})\cos 4\varphi\\
Q_{22}' &= \tfrac{1}{8}(3Q_{11}+3Q_{22}+2Q_{12}+4Q_{66})-\tfrac{1}{2}(Q_{11}-Q_{22})\cos 2\varphi+\tfrac{1}{8}(Q_{11}+Q_{22}-2Q_{12}-4Q_{66})\cos 4\varphi\\
Q_{12}' &= \tfrac{1}{8}(Q_{11}+Q_{22}+6Q_{12}-4Q_{66})-\tfrac{1}{8}(Q_{11}+Q_{22}-2Q_{12}-4Q_{66})\cos 4\varphi\\
Q_{16}' &= -\tfrac{1}{4}(Q_{11}-Q_{22})\sin 2\varphi-\tfrac{1}{8}(Q_{11}+Q_{22}-2Q_{12}-4Q_{66})\sin 4\varphi\\
Q_{26}' &= -\tfrac{1}{4}(Q_{11}-Q_{22})\sin 2\varphi+\tfrac{1}{8}(Q_{11}+Q_{22}-2Q_{12}-4Q_{66})\sin 4\varphi\\
Q_{66}' &= \tfrac{1}{8}(Q_{11}+Q_{22}-2Q_{12}+4Q_{66})-\tfrac{1}{8}(Q_{11}+Q_{22}-2Q_{12}-4Q_{66})\cos 4\varphi
\end{aligned} \qquad (4.13)$$

For the reduction of typing work, the next notation will be used:

$$\begin{aligned}
Q_{11}' &= U_1+U_2\cos 2\varphi+U_3\cos 4\varphi & U_1 &= \tfrac{1}{8}(3Q_{11}+3Q_{22}+2Q_{12}+4Q_{66})\\
Q_{22}' &= U_1-U_2\cos 2\varphi+U_3\cos 4\varphi & U_2 &= \tfrac{1}{2}(Q_{11}-Q_{22})\\
Q_{12}' &= U_4-U_3\cos 4\varphi & U_3 &= \tfrac{1}{8}(Q_{11}+Q_{22}-2Q_{12}-4Q_{66})\\
Q_{16}' &= -\tfrac{1}{2}U_2\sin 2\varphi-U_3\sin 4\varphi & U_4 &= \tfrac{1}{8}(Q_{11}+Q_{22}+6Q_{12}-4Q_{66})\\
Q_{26}' &= -\tfrac{1}{2}U_2\sin 2\varphi+U_3\sin 4\varphi & U_5 &= \tfrac{1}{8}(Q_{11}+Q_{22}-2Q_{12}+4Q_{66})\\
Q_{66}' &= U_5-U_3\cos 4\varphi
\end{aligned} \qquad (4.14)$$

4.3 Micromechanics

A composite material consists of different components with different properties. Micromechanics predicts the relation between the properties of the constituents and those of the composite material. The law of mixtures is the simplest relation for predicting micromechanic relations. With this rule, the composite property is calculated by the sum of the property of each constituent multiplied by its volume fraction.

Relations between composite densities and densities of the constituents can theoretically be calculated with the mixture rule:

$$
\begin{aligned}
&M_c = M_f + M_m \\
&V_c = V_f + V_m \\
&m_f + m_m = 1 \\
&v_f + v_m + v_v = 1 \\
&\rho_c = \frac{M_c}{V_c} = \frac{\rho_f V_f + \rho_m V_m}{V_c} = \rho_f v_f + \rho_m v_m \\
&= \frac{M_c}{\frac{M_f}{\rho_f} + \frac{M_m}{\rho_m} + V_v} = \frac{1}{\frac{m_f}{\rho_f} + \frac{m_m}{\rho_m} + \frac{V_v}{M_c}} = \frac{1}{\frac{m_f}{\rho_f} + \frac{m_m}{\rho_m} + \frac{v_v}{\rho_c}}
\end{aligned}
\qquad (4.15)
$$

Where:

M = mass
V = volume
m = mass fraction
v = volume fraction
ρ = density

If the fibre mass fraction is known, the glass volume fraction can be calculated with:

$$
v_{glass} = m_{glass} \cdot \frac{\rho_{SMC}}{\rho_{glass}} \qquad (4.16)
$$

The mixture rule can also be used to predict mechanical behaviour of composite materials by calculating by the sum of the strains or stresses of each constituent multiplied by its volume fraction.

$$
\begin{aligned}
&\sigma_i^c = v_f \sigma_i^f + v_m \sigma_i^m \\
&\varepsilon_i^c = v_f \varepsilon_i^f + v_m \varepsilon_i^m
\end{aligned}
\qquad (4.17)
$$

From these mixture rules, the following models for the longitudinal and the transversal Young's modulus are derived by assuming identical state of deformation or stress respectively:

$$
\begin{aligned}
&E_L = v_f E_f + v_m E_m \qquad \text{Parallel model [Voigt]} \\
&\frac{1}{E_T} = \frac{v_f}{E_f} + \frac{v_m}{E_m} \qquad \text{Series Model [Ruess]}
\end{aligned}
\qquad (4.18)
$$

In these models is assumed that the Poissons ratios of the matrix, fibres and composite are equal. This results in no interaction between the fibres and matrix perpendicular to the direction of the load. This is not realistic because in reality interaction perpendicular to the load does occur.

Halphin and Tsai have derived formulas for calculating mechanical constants of composites. With the formulas of Halphin and Tsai also mechanical constants of composites with unidirectional short fibres can be calculated. The general formula for calculating a property P of the composite from the properties P^f and P^m from the matrix and the fibres respectively is:

$$P = P_m \frac{1+\xi\mu v_f}{1-\mu v_f} \qquad \text{with} \quad \mu = \frac{P_f - P_m}{P_f + \xi P_m} \tag{4.19}$$

The value of ξ depends on the property and on the geometry and properties of the fibres. Values for ξ are given in the table 4.1.

P	P_f	P_m	ξ	Remarks
E_L	E_L^f	E_L^m	$2\frac{l}{d}$	l= fibre length, d= fibre diameter
E_T	E_T^f	E_T^m	∞	
ν_{LT}	ν_{LT}^f	ν_{LT}^m	$2\frac{a}{b}$	a and b are fibre dimensions of the cross section in the 1 and 2 direction respectively
G_{LT}	G_{LT}^f	G_{LT}^m	$\left(\frac{a}{b}\right)^{\sqrt{3}}$	
G_{TT}	G_{TT}^f	G_{TT}^m	$\frac{k_m}{k_m+2G_{TT}^m} = \frac{1}{3-4\nu_m}$ for isotrope matrix	$k = \frac{0.5(\sigma_2+\sigma_3)}{(\varepsilon_2+\varepsilon_3)}$ (transverse compression mod.)

Table 4.1

For the various mechanical components, the following formulas can be derived:

$$\begin{aligned}
E_T &= E_T^m \frac{1+2\frac{a}{b}\mu v_f}{1-\mu v_f} \qquad \text{with} \quad \mu = \frac{E_T^f - E_T^m}{E_T^f + 2\frac{a}{b}E_T^m} \\
E_L &= E_L^m \frac{1+2\frac{l}{d}\mu v_f}{1-\mu v_f} \qquad \text{with} \quad \mu = \frac{E_L^f - E_L^m}{E_L^f + 2\frac{l}{d}E_L^m} \\
G_{LT} &= G_{LT}^m \frac{1+\left(\frac{a}{b}\right)^{\sqrt{3}}\mu v_f}{1-\mu v_f} \qquad \text{with} \quad \mu = \frac{G_{LT}^f - G_{LT}^m}{G_{LT}^f + \left(\frac{l}{d}\right)^{\sqrt{3}}G_{LT}^m} \\
\nu_{LT} &= \nu_{LT}^m \frac{1+\infty\mu v_f}{1-\mu v_f} \qquad \text{with} \quad \mu = \frac{\nu_{LT}^f - \nu_{LT}^m}{\nu_{LT}^f + \infty\nu_{LT}^m}
\end{aligned} \tag{4.20}$$

$$\begin{aligned}
&\Rightarrow \nu_{LT} = \nu_{LT}^m \frac{\left(1+\infty v_f\right)\nu_{LT}^f + \infty v_m \nu_{LT}^m}{v_m \nu_{LT}^f + \left(\infty + v_f\right)\nu_{LT}^m} \approx \nu_{LT}^m \frac{\infty v_f \nu_{LT}^f + \infty v_m \nu_{LT}^m}{\infty \nu_{LT}^m} \\
&\Rightarrow \nu_{LT} \approx v_f \nu_{LT}^f + v_m \nu_{LT}^m
\end{aligned} \tag{4.21}$$

4.4 Expansion of composites

During and after the moulding of an SMC, temperature change, polymerisation shrinkage and LPA effects cause volume changes of the matrix. Also the fibre volume changes due to thermal effects. How the separate expansions of the individual components influence the residual expansion of the composite is explained below. In figure 4.3 a one dimensional situation is depicted.

The separate components exhibit a free expansional strain.

$$\varepsilon_1^e = \frac{\Delta l_1}{l} \qquad \varepsilon_2^e = \frac{\Delta l_2}{l} \tag{4.22}$$

In the composite, the two components are forced to undergo the same residual strain. The different free expansional strains of the two components lead to internal stresses. The residual strain in each component is the sum of the free expansional strain and the strain caused by the internal stress.

$$\varepsilon_r = \frac{\Delta l_r}{l} = \varepsilon_1^e + \varepsilon_1^\sigma = \varepsilon_2^e + \varepsilon_2^\sigma \Rightarrow \qquad (4.23)$$

$$\varepsilon_1^\sigma = \varepsilon_r - \varepsilon_1^e \qquad \varepsilon_2^\sigma = \varepsilon_r - \varepsilon_2^e$$

With balance of forces:

$$F_1 + F_2 = 0 \Rightarrow v_1\sigma_1 + v_2\sigma_2 = 0 \qquad (4.24)$$

and

$$\sigma_1 = E_1\varepsilon_1 \qquad \sigma_2 = E_2\varepsilon_2 \qquad (4.25)$$

the residual strain of the composite in longitudinal direction can be expressed as:

$$\varepsilon^r = \frac{v_1E_1\varepsilon_1^e + v_2E_2\varepsilon_1^e}{v_1E_1 + v_2E_2} \qquad (4.26)$$

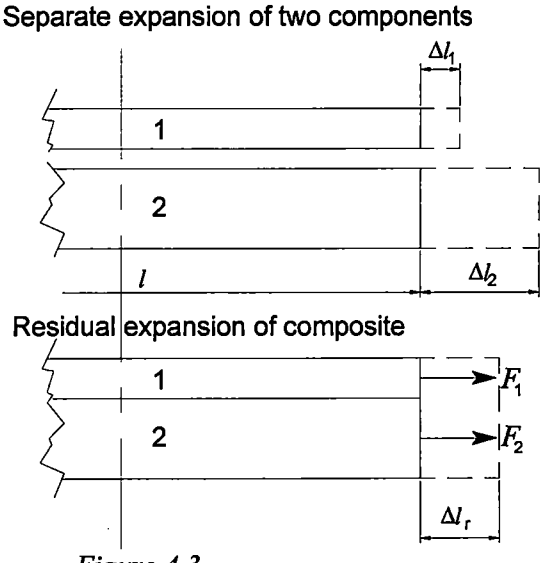

Figure 4.3

For unidirectional composites with continuous fibres this formula can be used to approximate the residual expansion in the longitudinal direction. The parallel model is an approximation because in reality also residual stresses occur in transversal direction. A formula for the transversal expansion of the composite can be derived when is assumed that the free expansional strain is the same in all directions.

$$\varepsilon_T^r = v_1\varepsilon_1^r + v_2\varepsilon_2^r = v_1(\varepsilon_1^e - \frac{v_1}{E_1}\sigma_1) + v_2(\varepsilon_2^e - \frac{v_2}{E_2}\sigma_2) \qquad (4.27)$$

With $\sigma_1 = E_1(\varepsilon_L^r - \varepsilon_1^e)$ and *(4.26)*, this becomes:

$$\varepsilon_T^r = v_1(1+v_1)\varepsilon_1 + v_2(1+v_2)\varepsilon_2 - (v_1v_1 + v_2v_2)\varepsilon^r \qquad \varepsilon^r = \text{the longitudinal residual strain}$$

These formulas for the relations between the expansion of the fibres, matrix and the composite are known as the formulas of Shapery. For composite materials f and m for fibre and matrix replace the indices 1, and 2 respectively.

$$\varepsilon_L = \frac{v_fE_f\varepsilon_f + v_mE_m\varepsilon_m}{v_fE_f + v_mE_m} \qquad \text{[Shapery]} \qquad (4.28)$$

$$\varepsilon_T = v_f(1+v_f)\varepsilon_f + v_m(1+v_m)\varepsilon_m - (v_fv_f + v_mv_m)\varepsilon_L$$

The transversal expansion of unidirectional short fibre composites can be estimated with Shapery's formula because ε_T is not a sensitive function of the *l/d* ratio for short fibre composites. It is primarily the longitudinal expansion ε_L, which is sensitive to the *l/d* ratio. Halphin has given the following formula for estimating the longitudinal expansion of oriented short fiber composites. In this equation the mean of the upper and lower bounds on ε_L, calculated parallel- and series model, are taken [Halphin].

$$\varepsilon_L = \bar{\varepsilon} + \left(\frac{\overline{E\varepsilon}}{\overline{E}} - \bar{\varepsilon} \right) \frac{\frac{1}{E_{L(-)}} - \frac{1}{E_L}}{\frac{1}{E_{L(-)}} - \frac{1}{E_{L(+)}}} \qquad (4.29)$$

$$\bar{\varepsilon} = (v_f \varepsilon_f + v_m \varepsilon_m)$$

$$\overline{E} = (v_f E_f + v_m E_m)$$

$\frac{\overline{E\varepsilon}}{\overline{E}} = \varepsilon_L$ for an u.d. material with continuous fibres [Shapery]

E_L follows from the Halphin - Tsai equation [...]

$$\frac{1}{E_{L(-)}} = \frac{v_f}{E_f} + \frac{v_m}{E_m}$$ Lower limit for E_L follows from series connection model of Reuss (4.30)

$$\frac{1}{E_{L(+)}} = \frac{1}{v_f E_f + v_m E_m}$$ Upper limit for E_L follows from parallel connection model of Voigt

4.5 Laminate theory

Until now, the stress-strain behaviour of unidirectional fibre reinforced composites has been described. Mechanical properties of laminates that consist of unidirectional plies with fibres oriented in various directions can be predicted with the laminate theory. In this paragraph first a short description of this laminate theory is given.
Furthermore an explanation is given how the laminate theory can be used to calculate the expansion of the laminate as function of the expansion of the individual unidirectional plies. Then in the next paragraph is explained how this theory can be applied to predict the mechanical properties and the expansion of sheet moulding compounds.

In this description of the laminate theory an xyz co-ordinate system is coupled to the laminate. The xy-plane is the middle plane of the laminate. To the individual plies, a contracted co-ordinate system is coupled. A ply in a laminate rotated in the xy-plane as depicted in figure 4.2.

In paragraph 4.2 is explained that the stress-strain behaviour of unidirectional fibre reinforced plies can be described with the reduced stiffness matrix Q *(4.9)*. Behaviour of the individual plies in the x- and y directions of the ply can be calculated by determining the reduced stiffness matrix Q' after a rotation transformation in the 1 2-plane as explained in paragraph 4.2. In the formulas 4.13, φ must be replaced by $-\theta$. With the stress-strain behaviour of the separate unidirectional plies and the balance of momentum and balance of forces, the following relation between load and deformation of the laminate can be derived.

$$\begin{pmatrix} N_x \\ N_y \\ N_{xy} \\ M_x \\ M_y \\ M_{xy} \end{pmatrix} = \begin{pmatrix} A_{11} & A_{12} & A_{13} & B_{11} & B_{12} & B_{13} \\ & A_{22} & A_{23} & B_{21} & B_{22} & B_{23} \\ & & A_{33} & B_{31} & B_{32} & B_{33} \\ & & & D_{11} & D_{12} & D_{13} \\ & & & & D_{22} & D_{23} \\ & & & & & D_{33} \end{pmatrix} \cdot \begin{pmatrix} \varepsilon_x^{\,0} \\ \varepsilon_y^{\,0} \\ \varepsilon_{yz}^{\,0} \\ \kappa_x \\ \kappa_y \\ \kappa_{xy} \end{pmatrix} \qquad (4.31)$$

N and M are stress resultants and moment resultants respectively, defined as:

$$N_x = \int_{-\frac{h}{2}}^{\frac{h}{2}} \sigma_x dz \quad N_y = \int_{-\frac{h}{2}}^{\frac{h}{2}} \sigma_y dz \quad N_{xy} = \int_{-\frac{h}{2}}^{\frac{h}{2}} \sigma_{xy} dz$$

$$M_x = \int_{-\frac{h}{2}}^{\frac{h}{2}} \sigma_x dz \quad M_y = \int_{-\frac{h}{2}}^{\frac{h}{2}} \sigma_y dz \quad M_{xy} = \int_{-\frac{h}{2}}^{\frac{h}{2}} \sigma_{xy} dz \qquad (4.32)$$

ε^0 = strain of the midplane of the laminate
κ = Curvature of the laminate

A = extensional stiffness matrix:

$$A_{ij} = \sum_{k=1}^{n} \left(Q_{ij}'\right)_k (z_k - z_{k-1}) \qquad (4.33)$$

B = coupling stiffness matrix:

$$B_{ij} = \tfrac{1}{2} \sum_{k=1}^{n} \left(Q_{ij}'\right)_k \left(z_k^{\,2} - z_{k-1}^{\,2}\right) \qquad (4.34)$$

D = bending stiffness matrix

$$D_{ij} = \tfrac{1}{3} \sum_{k=1}^{n} \left(Q_{ij}'\right)_k \left(z_k^{\,3} - z_{k-1}^{\,3}\right) \qquad (4.35)$$

n = the number of plies
z = upper z co - ordinate of k'th ply

The matrices A, B and D are symmetric matrices. The extensional stiffness matrix A describes the relation of load and deformation in the plane of the laminate. The bending stiffness matrix D describes the bending and torsion stiffness of the laminate. The coupling matrix B describes the relations between loads in the plane and bending and torsion deformation and the relations between the moment resultants and deformations in the plane.

4.6 Expansion of laminates

As explained in paragraph 3.3.5, temperature change, polymerisation shrinkage and LPA effects cause volume changes of the matrix. Also the fibre volume changes due to thermal effects. The different expansional strains of the fibres and matrix and the anisotropy result in different expansional strains in the longitudinal and transversal direction of the unidirectional ply. For calculation of the residual expansion of the laminate from the separate free expansions of the individual plies, the one dimensional model figure 4.2 can be used.

$$\varepsilon_r = \frac{\Delta l_r}{l} = \varepsilon_1^e + \varepsilon_1^\sigma = \varepsilon_2^e + \varepsilon_2^\sigma \Rightarrow \qquad (4.36)$$

$$\varepsilon_1^\sigma = \varepsilon_r - \varepsilon_1^e \qquad \varepsilon_2^\sigma = \varepsilon_r - \varepsilon_2^e$$

With balance of forces:

$$\begin{pmatrix} N_x^e \\ N_y^e \\ N_{xy}^e \end{pmatrix} = \sum_{k=1}^{n} \int_{z_{k-1}}^{z_k} \begin{pmatrix} Q'_{11} & Q'_{12} & Q'_{16} \\ & Q'_{22} & Q'_{26} \\ & & Q'_{66} \end{pmatrix}_k \begin{pmatrix} \varepsilon_1'^r - \varepsilon_1'^e \\ \varepsilon_1'^r - \varepsilon_1'^e \\ 0 \end{pmatrix}_k dz = \begin{pmatrix} 0 \\ 0 \\ 0 \end{pmatrix} \qquad (4.37)$$

These strain components can be transformed from the ply- to the laminate-axis with *(4.12)*:

$$\begin{pmatrix} N_x^e \\ N_y^e \\ N_{xy}^e \end{pmatrix} = \sum_{k=1}^{n} \int_{z_{k-1}}^{z_k} \begin{pmatrix} Q'_{11} & Q'_{12} & Q'_{16} \\ & Q'_{22} & Q'_{26} \\ & & Q'_{66} \end{pmatrix}_k \begin{pmatrix} \cos^2\theta & \sin^2\theta & -\sin\theta\cos\theta \\ \sin^2\theta & \cos^2\theta & \sin\theta\cos\theta \\ 2\sin\theta\cos\theta & -2\sin\theta\cos\theta & \cos^2\theta - \sin^2\theta \end{pmatrix}_k \begin{pmatrix} \varepsilon_1^r - \varepsilon_1^e \\ \varepsilon_1^r - \varepsilon_1^e \\ 0 \end{pmatrix}_k dz = \begin{pmatrix} 0 \\ 0 \\ 0 \end{pmatrix}$$

Or:

$$\mathbf{0} = \sum \int Q'_k \, T_k^{-\mathrm{T}} \begin{pmatrix} \varepsilon_1^r - \varepsilon_1^e \\ \varepsilon_2^r - \varepsilon_2^e \\ 0 \end{pmatrix}_k dz \quad \Rightarrow \qquad (4.38)$$

$$\mathbf{0} = \sum \int Q'_k \, T_k^{-T} \begin{pmatrix} \varepsilon_1^r \\ \varepsilon_2^r \\ 0 \end{pmatrix} dz - \sum \int Q'_k \, T_k^{-\mathrm{T}} \begin{pmatrix} \varepsilon_1^e \\ \varepsilon_2^e \\ 0 \end{pmatrix}_k dz \quad \Rightarrow$$

$$\sum \int Q'_k \, T_k^{-T} \begin{pmatrix} \varepsilon_1^r \\ \varepsilon_2^r \\ 0 \end{pmatrix} dz = \sum \int Q'_k \, T_k^{-\mathrm{T}} \begin{pmatrix} \varepsilon_1^e \\ \varepsilon_2^e \\ 0 \end{pmatrix}_k dz \quad \Rightarrow \sum \int Q'_k \, dz \begin{pmatrix} \varepsilon_x^r \\ \varepsilon_y^r \\ 0 \end{pmatrix} = \sum \int Q'_k \, T_k^{-\mathrm{T}} \begin{pmatrix} \varepsilon_1^e \\ \varepsilon_2^e \\ 0 \end{pmatrix}_k dz \quad \Rightarrow$$

With *(4.33)*:

$$A \begin{pmatrix} \varepsilon_x^r \\ \varepsilon_y^r \\ 0 \end{pmatrix} = \sum \int Q'_k \, T_k^{-\mathrm{T}} \begin{pmatrix} \varepsilon_1^e \\ \varepsilon_2^e \\ 0 \end{pmatrix}_k dz \quad \Rightarrow \begin{pmatrix} \varepsilon_x^r \\ \varepsilon_y^r \\ 0 \end{pmatrix} = A^{-1} \sum \int Q'_k \, T_k^{-\mathrm{T}} \begin{pmatrix} \varepsilon_1^e \\ \varepsilon_2^e \\ 0 \end{pmatrix}_k dz \qquad (4.39)$$

4.7 Application of theory on Sheet Moulding Compounds

SMC's are composites reinforced with random oriented short fibres. Mechanical properties of SMC can be calculated by imagining the composite as a laminate of infinitely many plies of infinitely small thickness with fibres oriented in all directions.
Mechanical properties of the unidirectional short fibre plies can be calculated with the formulas of Halphin and Tsai, described in paragraph 4.3. Then the properties of the SMC can be calculated with the laminate theory as follows.

If the laminate is imagined to consists of very thin orthotropic layers, the summations in *(4.33)*, *(4.34)* and *(4.35)* can be replaced by integrals. Because the plies are imagined to be identical and random oriented, θ is independent of z:

$$A = \frac{1}{\pi} \int_{-\frac{\pi}{2}}^{\frac{\pi}{2}} Q' \, d\theta \int_{-\frac{h}{2}}^{\frac{h}{2}} dz = \frac{h}{\pi} \int_{-\frac{\pi}{2}}^{\frac{\pi}{2}} Q' \, d\theta \qquad (4.40)$$

$$B = \frac{1}{\pi} \int_{-\frac{\pi}{2}}^{\frac{\pi}{2}} Q' \, d\theta \int_{-\frac{h}{2}}^{\frac{h}{2}} z \, dz = 0 \qquad (4.41)$$

$$D=\frac{1}{\pi}\int_{-\frac{\pi}{2}}^{\frac{\pi}{2}}Q'\,d\theta\int_{-\frac{h}{2}}^{\frac{h}{2}}z^2\,dz=\frac{h^3}{12\pi}\int_{-\frac{\pi}{2}}^{\frac{\pi}{2}}Q'\,d\theta=\frac{h^2}{12\pi}A \tag{4.42}$$

Because $\int_{-\frac{\pi}{2}}^{\frac{\pi}{2}}\cos 2n\pi d\theta=\int_{-\frac{\pi}{2}}^{\frac{\pi}{2}}\sin 2n\pi d\theta=0$ for $n=1,2,...\Rightarrow$

$$A=h\begin{pmatrix}\frac{1}{8}(3Q_{11}+3Q_{22}+2Q_{12}+4Q_{66}) & \frac{1}{8}(Q_{11}+Q_{22}+6Q_{12}-4Q_{66}) & 0\\ \frac{1}{8}(Q_{11}+Q_{22}+6Q_{12}-4Q_{66}) & \frac{1}{8}(3Q_{11}+3Q_{22}+2Q_{12}+4Q_{66}) & 0\\ 0 & 0 & \frac{1}{8}(Q_{11}+Q_{22}-2Q_{12}+4Q_{66})\end{pmatrix} \tag{4.43}$$

This can be derived from the relation between Q and Q' *(4.13)*. With the simplified notation of *(4.14)*, this becomes:

$$A=h\cdot\begin{pmatrix}U_1 & U_4 & 0\\ U_4 & U_1 & 0\\ 0 & 0 & U_5\end{pmatrix} \tag{4.44}$$

The expansion in longitudinal and transversal direction of ud-plies with unidirectional short fibres can be calculated from the expansion of the matrix and fibres with the formulas of Shapery and Halphin *(4.20)*. *(4.21)*. The expansion of the SMC can be calculated from the longitudinal and transversal expansion of the ud-ply by again assuming a laminate, consisting of many random oriented thin plies with unidirectional short fibres. Because all plies are assumed to be identical, the free expansional strains of the plies are the same:

$$\begin{pmatrix}\varepsilon_x^r\\ \varepsilon_y^r\\ 0\end{pmatrix}=A^{-1}\sum\int Q'_k\,T_k^{-\mathrm{T}}\begin{pmatrix}\varepsilon_1^e\\ \varepsilon_2^e\\ 0\end{pmatrix}_k dz=A^{-1}\left\{\varepsilon_1^e\sum\int Q'_k\begin{pmatrix}\cos^2\theta\\ \sin^2\theta\\ 2\sin\theta\cos\theta\end{pmatrix}_k dz+\varepsilon_2^e\sum\int Q'_k\begin{pmatrix}\sin^2\theta\\ \cos^2\theta\\ -2\sin\theta\cos\theta\end{pmatrix}_k dz\right\} \tag{4.45}$$

If random orientation is assumed, the summations in *(4.45)* can be changed into integrals:

$$\begin{pmatrix}\varepsilon_x^r\\ \varepsilon_y^r\\ 0\end{pmatrix}=\frac{h}{\pi}A^{-1}\int_{-\frac{\pi}{2}}^{\frac{\pi}{2}}Q'_k\,T_k^{-\mathrm{T}}\begin{pmatrix}\varepsilon_1^e\\ \varepsilon_2^e\\ 0\end{pmatrix}_k d\theta=\frac{h}{\pi}A^{-1}\left\{\varepsilon_1^e\int_{-\frac{\pi}{2}}^{\frac{\pi}{2}}Q'_k\begin{pmatrix}\cos^2\theta\\ \sin^2\theta\\ 2\sin\theta\cos\theta\end{pmatrix}_k d\theta+\varepsilon_2^e\int_{-\frac{\pi}{2}}^{\frac{\pi}{2}}Q'_k\begin{pmatrix}\sin^2\theta\\ \cos^2\theta\\ -2\sin\theta\cos\theta\end{pmatrix}_k d\theta\right\}$$

with:

$$\begin{aligned}Q'_{11}&=U_1+U_2\cos 2\theta+U_3\cos 4\theta\\ Q'_{22}&=U_1-U_2\cos 2\theta+U_3\cos 4\theta\\ Q'_{12}&=U_4-U_3\cos 4\theta\\ Q'_{16}&=\tfrac{1}{2}U_2\sin 2\theta+U_3\sin 4\theta\\ Q'_{26}&=\tfrac{1}{2}U_2\sin 2\theta-U_3\sin 4\theta\\ Q'_{66}&=U_5-U_3\cos 4\theta\end{aligned} \tag{4.46}$$

can be derived that:

$$\begin{pmatrix}\varepsilon_x^r\\ \varepsilon_y^r\\ 0\end{pmatrix}=\frac{h}{\pi}A^{-1}\left\{\varepsilon_1^e\int_{-\frac{\pi}{2}}^{\frac{\pi}{2}}Q_k'\begin{pmatrix}\cos^2\theta\\ \sin^2\theta\\ 2\sin\theta\cos\theta\end{pmatrix}_k d\theta+\varepsilon_2^e\int_{-\frac{\pi}{2}}^{\frac{\pi}{2}}Q_k'\begin{pmatrix}\sin^2\theta\\ \cos^2\theta\\ -2\sin\theta\cos\theta\end{pmatrix}_k d\theta\right\} \tag{4.47}$$

$$=\frac{h}{2}A^{-1}\left\{\begin{pmatrix}U_1+U_2+U_4\\ U_1+U_2+U_4\\ 0\end{pmatrix}\varepsilon_L^e+\begin{pmatrix}U_1-U_2+U_4\\ U_1-U_2+U_4\\ 0\end{pmatrix}\varepsilon_T^e\right\}$$

With *(4.43)* the extensional stiffness matrix A was determined of the random oriented laminate:

$$A=h\cdot\begin{pmatrix}U_1 & U_4 & 0\\ U_4 & U_1 & 0\\ 0 & 0 & U_5\end{pmatrix}\qquad\Rightarrow A^{-1}=\frac{1}{h\left(U_1^2-U_4^2\right)}\begin{pmatrix}U_1 & -U_4 & 0\\ -U_4 & U_1 & 0\\ 0 & 0 & \frac{U_1^2-U_4^2}{U_5}\end{pmatrix} \tag{4.48}$$

With *(4.47)* and *(4.48)* the following relation for the residual strain of the random oriented laminate is obtained:

$$\begin{pmatrix}\varepsilon_x^r\\ \varepsilon_y^r\\ 0\end{pmatrix}=\frac{1}{2\left(U_1+U_4\right)}\left\{\begin{pmatrix}U_1+U_2+U_4\\ U_1+U_2+U_4\\ 0\end{pmatrix}\varepsilon_L^e+\begin{pmatrix}U_1-U_2+U_4\\ U_1-U_2+U_4\\ 0\end{pmatrix}\varepsilon_T^e\right\} \tag{4.49}$$

or:

$$\varepsilon^r=\frac{U_1+U_2+U_4}{2\left(U_1+U_4\right)}\varepsilon_L^e+\frac{U_1-U_2+U_4}{2\left(U_1+U_4\right)}\varepsilon_T^e \tag{4.50}$$

With *(4.14)* this relation can be expressed in the components of the reduced stiffness matrix *Q*:

$$\varepsilon^r=\frac{Q_{11}+Q_{12}}{Q_{11}+Q_{22}+2Q_{12}}\varepsilon_L^e+\frac{Q_{22}+Q_{12}}{Q_{11}+Q_{22}+2Q_{12}}\varepsilon_T^e \tag{4.51}$$

Now with 4.10 the residual strain of the random oriented laminate can be expressed as function of the free expansional strain and the engineering constants of the unidirectional ply:

$$\varepsilon^r=\frac{E_L+\nu_{LT}E_T}{E_L+E_T+2\nu_{LT}E_T}\varepsilon_L^e+\frac{E_T(1+\nu_{LT})}{E_L+E_T+2\nu_{LT}E_T}\varepsilon_T^e \tag{4.52}$$

or because:

$$\nu_{LT}E_T=\nu_{TL}E_L\Rightarrow\qquad\varepsilon^r=\frac{E_L(1+\nu_{TL})}{E_L+E_T+2\nu_{LT}E_T}\varepsilon_L^e+\frac{E_T(1+\nu_{LT})}{E_L+E_T+2\nu_{LT}E_T}\varepsilon_T^e \tag{4.53}$$

Literature

1. Halphin, J.C., 'Stiffness and expansion estimates for oriented short fiber composites', *J. Composite materials*, Vol. 3, October 1969, p. 732
2. Nijhof, A.H.J., *Mechanica van composietmaterialen,* TU-Delft dictate, 1994-95
3. Tsai, S.W., *Composites design*, fourth edition, Think composites, USA, 1988
4. Tsai, S.W., Hahn, T., *Introduction to composite materials*, Technomic Publishing Company, Inc., USA, 1980